

# Kinematics of syn- and post-exhumational shear zones at Lago di Cignana (Western Alps, Italy): constraints on the exhumation of Zermatt–Saas (ultra)high-pressure rocks and deformation along the Combin Fault and Dent Blanche Basal Thrust

Frederik Kirst<sup>1</sup> · Bernd Leiss<sup>2</sup>

Received: 26 April 2015 / Accepted: 28 February 2016 / Published online: 21 March 2016  
© Springer-Verlag Berlin Heidelberg 2016

**Abstract** Kinematic analyses of shear zones at Lago di Cignana in the Italian Western Alps were used to constrain the structural evolution of units from the Piemont–Ligurian oceanic realm (Zermatt–Saas and Combin zones) and the Adriatic continental margin (Dent Blanche nappe) during Palaeogene syn- and post-exhumational deformation. Exhumation of Zermatt–Saas (U)HP rocks to approximately lower crustal levels at ca. 39 Ma occurred during normal-sense top-(S)E shearing under epidote–amphibolite-facies conditions. Juxtaposition with the overlying Combin zone along the Combin Fault at mid-crustal levels occurred during greenschist-facies normal-sense top-SE shearing at ca. 38 Ma. The scarcity of top-SE kinematic indicators in the hanging wall of the Combin Fault probably resulted from strain localization along the uppermost Zermatt–Saas zone and obliteration by subsequent deformation. A phase of dominant pure shear deformation around 35 Ma affected units in the direct footwall and hanging wall of the Combin Fault. It is interpreted to reflect NW–SE crustal elongation during updoming of the nappe stack as a result of underthrusting of European continental margin units and the onset of continental collision. This phase was partly accompanied and followed by ductile bulk top-NW shearing, especially at higher structural levels, which transitioned into semi-ductile to brittle normal-sense top-NW deformation due to Vanzone phase folding from ca. 32 Ma onwards. Our structural observations suggest that

syn-exhumational deformation is partly preserved within units and shear zones exposed at Lago di Cignana but also that the Combin Fault and Dent Blanche Basal Thrust experienced significant post-exhumational deformation reworking and overprinting earlier structures.

**Keywords** Western Alps · Lago di Cignana · Zermatt–Saas zone · Combin Fault · Dent Blanche Basal Thrust · Syn- and post-exhumational deformation

## Introduction

Deformation in Alpine-type orogens results from cycles of subduction and accretion, exhumation, and continental collision. Continental and oceanic units can be subducted to and exhumed back from (ultra)high-pressure ((U)HP) depths. During subsequent nappe stacking, crustal units that experienced such extreme conditions are juxtaposed with lower-pressure units along major tectonic contacts. Deformation structures associated with initial exhumation from (U)HP conditions are often obliterated by later deformation phases resulting from nappe stacking, reactivation of shear zones and tectonic contacts, and continental collision. Accordingly, it is often controversial whether observed structures resulted from exhumation-related deformation or merely represent younger deformation phases. A classic example for oceanic (U)HP conditions and the discussion of exhumation-related deformation is the Zermatt–Saas zone in the Swiss–Italian Western Alps with its associated UHP sliver, the Lago di Cignana unit (e.g. Reinecke 1991; Forster et al. 2004; Groppo et al. 2009) in the western Valtourneche of Italy. These units are derived from the Piemont–Ligurian oceanic realm (South Penninic palaeogeographic domain; Fig. 1a), which experienced a Palaeogene cycle of

✉ Frederik Kirst  
freddi.kirst@gmail.com

<sup>1</sup> Steinmann-Institut, University of Bonn, Meckenheimer Allee 169, 53115 Bonn, Germany

<sup>2</sup> Geowissenschaftliches Zentrum, University of Göttingen, Goldschmidtstr. 3, 37077 Göttingen, Germany

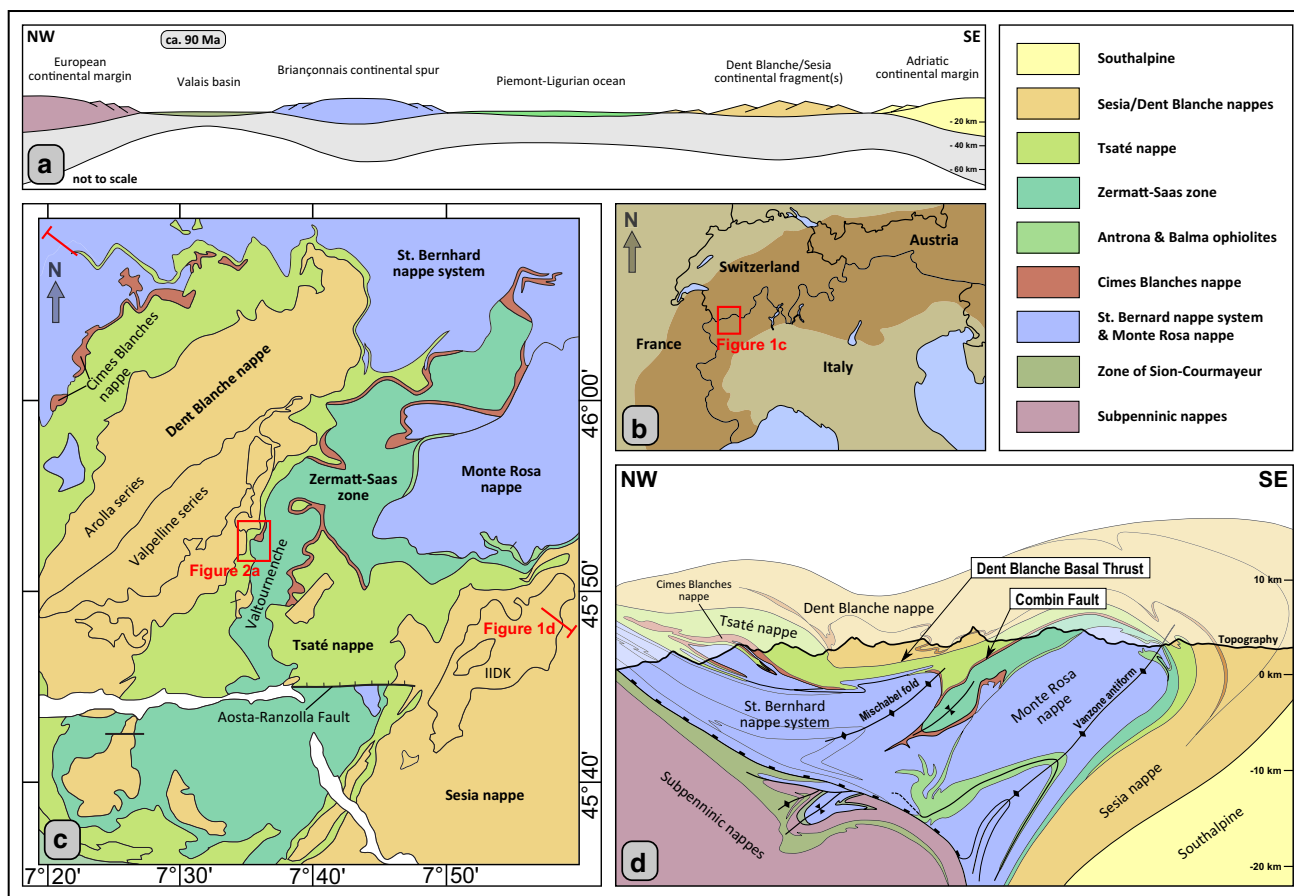


**Fig. 1** **a** Late Cretaceous palaeogeography before the onset of Alpine subduction; the Zermatt–Saas zone and Tsaté nappe are derived from the Piemont–Ligurian oceanic realm; the Dent Blanche/Sesia nappe system originated from continental fragments rifted off the Adriatic continental margin during the Jurassic. **b** Sketch map of the European

Alps with location of the tectonic map. **c** Tectonic map of the Peninic units in the Swiss–Italian Western Alps after Steck et al. (1999) and Pleuger et al. (2007) with location of the geological map in **a**. **d** Schematic cross section through the Western Alps; after Escher et al. (1993) and Pleuger et al. (2007)

subduction, exhumation, and collision. The Zermatt–Saas zone is situated in the footwall of the Combain zone and its basal tectonic contact, the Combain Fault, the significance of which for the exhumation of the underlying (U)HP rocks has been controversially discussed in the literature. The large difference in metamorphic grade between the eclogite-facies Zermatt–Saas zone in the footwall (e.g. Bearth 1967; Dal Piaz and Ernst 1978) and the greenschist- to blueschist-facies Combain zone in the hanging wall (e.g. Dal Piaz 1965) has led many authors to interpret the Combain Fault as a top-SE normal fault that accommodated exhumation of Zermatt–Saas (U)HP rocks (e.g. Ballèvre and Merle 1993; Reddy et al. 1999, 2003; Wheeler et al. 2001). This interpretation has been questioned by several authors due to the occurrence of abundant greenschist-facies top-NW kinematic indicators along the Combain Fault and within the Combain zone. Ballèvre and Merle (1993) suggested that a Combain normal fault was overprinted by post-exhumational top-NW thrusting erasing earlier top-SE structures,

which was then followed by late-stage top-SE backfolding. Ring (1995) proposed that the Combain Fault represents an Eocene out-of-sequence thrust also overprinted by later top-SE backshearing. Froitzheim et al. (2006) and Pleuger et al. (2007) interpreted the Combain Fault as an extraction fault that formed due to extraction and subsequent out-of-sequence thrusting of the Dent Blanche nappe. Reddy et al. (2003) proposed on the basis of syn-kinematic Ar–Ar and Rb–Sr ages that top-SE shearing within the Combain zone was dominant during exhumation of the Zermatt–Saas zone but also overlapped and was partly coeval with the activity of top-NW shear zones due to a significant pure shear component. Whereas the nature of the Combain Fault is still a matter of discussion, the Dent Blanche Basal Thrust (DBBT) separating the continental Dent Blanche nappe from the underlying Combain zone is usually interpreted to represent a major Alpine thrust of mainly Eocene age (e.g. Mazurek 1986; Oberhänsli and Bucher 1987; Ring 1995; Pleuger et al. 2007), which was most likely reactivated

during NW- and SE-vergent normal-sense shearing (Wust and Silverberg 1989; Reddy et al. 2003; Forster et al. 2004). In the Lago di Cignana area, both tectonic contacts, the Combin Fault and the DBBT, are well-exposed. This locality has been the site of many studies due to the occurrence of metabasic and metasedimentary UHP lithologies hosting coesite and microdiamond (Reinecke 1991; Frezzotti et al. 2011), and numerous studies have been carried out on the petrological and geochronological evolution of these rocks (e.g. Reinecke 1998; Amato et al. 1999; Lapen et al. 2003; Groppo et al. 2009). Studies dealing with structural aspects of this area comprise the work of Van der Klauw et al. (1997) who linked deformation structures to the exhumation path and Ballèvre and Merle (1993), Ring (1995), and Reddy et al. (2003) who included the Lago di Cignana area in their regional studies. Detailed mapping and structural work by Forster et al. (2004) within and around the UHP Lago di Cignana unit clarified the relations between UHP and HP rocks and put constraints on their structural evolution. In order to test the different models and geometries proposed for the structural evolution of the exposed nappe stack in this area and to constrain the kinematic evolution and nature of the two major tectonic contacts, the Combin Fault and the DBBT, we performed kinematic analyses on meso- and microscopic deformation structures across all structural levels, from Zermatt–Saas (U)HP rocks in the footwall of the Combin Fault across the Combin zone to mylonites in the hanging wall of the DBBT. The aim of this work is to constrain syn- and post-exhumational deformation along the tectonic contacts in the course of progressive Alpine orogeny and to clarify the significance of post-exhumational shearing events.

## Geological setting

The Swiss–Italian Western Alps consist of a stack of continental and oceanic units (Fig. 1b; e.g. Argand 1909; Steck et al. 1999), which are derived from different palaeogeographic domains (Fig. 1a). During the Late Cretaceous, before the onset of Alpine subduction, these included from northwest to southeast the European continental margin (Sub-Penninic domain), the Valais oceanic basin (North Penninic domain), the Briançonnais continental spur (Middle Penninic domain), the Piemonte–Ligurian oceanic realm (South Penninic domain), the Adriatic continental margin (Austroalpine domain), and associated ocean-continent transition zones (e.g. Stampfli et al. 2002; Schmid et al. 2004; Handy et al. 2010; Beltrando et al. 2014). In the course of SE-directed subduction during the Late Cretaceous–Palaeogene, crustal slices and partly mantle material from these different domains were progressively accreted to the Adriatic margin.

The study area is located in the Italian Western Alps where oceanic and continental units of the Piemonte–Ligurian domain and the Adriatic ocean-continent transition are exposed (Fig. 1b, c). The structurally highest unit is the Dent Blanche/Sesia nappe system, which is interpreted to originate from one or more continental fragments that were separated from the Adriatic continental margin during Jurassic rifting (Froitzheim et al. 1996; Dal Piaz et al. 2001). The Dent Blanche and Sesia nappes consist of Palaeozoic basement and remnants of Permo-Mesozoic cover sequences. The basement of the Dent Blanche nappe is subdivided into two units, the Arolla and Valpelline series (Argand 1906). The Arolla series consists of Permian granitoids and gabbros (Bussy et al. 1998; Monjoie et al. 2005), whereas the Valpelline series comprises pre-Alpine amphibolite- to granulite-facies metasediments (Gardien et al. 1994). Permo-Mesozoic cover rocks (Ciarapica et al. 2010), often referred to as Roisan zone (Ballèvre and Kienast 1987), comprise breccias, marbles, and quartzites. They occur on top of the Arolla series and along major shear zones (e.g. Manzotti 2011). The Alpine overprint within the Dent Blanche/Sesia nappe system increases from northwest to southeast which is consistent with SE-directed subduction and accretion of the units. The Dent Blanche nappe reached blueschist-facies conditions of ca. 1.4–1.6 GPa and 450–520 °C and shows a pervasive greenschist-facies overprint along shear zones (Ballèvre et al. 1986; Oberhänsli and Bucher 1987; Angiboust et al. 2014; Manzotti et al. 2014). The Sesia nappe experienced eclogite-facies conditions around 2.0 GPa and 550 °C (e.g. Lardeaux and Spalla 1991; Regis et al. 2014). High-pressure metamorphism in the Sesia nappe occurred during the Late Cretaceous at ca. 70–65 Ma (e.g. Inger et al. 1996; Rubatto et al. 1999) but may have started as early as ca. 85 Ma with distinct pressure peaks within different subunits (Rubatto et al. 2011; Regis et al. 2014). Rb–Sr geochronology on Arolla and Valpelline series rocks by Angiboust et al. (2014) yielded ages of ca. 58 Ma for Valpelline mylonites from within the Dent Blanche nappe and ca. 48–43 Ma for Arolla mylonites at its base. These have been interpreted to reflect the formation of blueschist-facies fabrics in the analysed samples. The basal tectonic contact of the Dent Blanche nappe towards the underlying Combin zone is the Dent Blanche Basal Thrust (DBBT). The Combin zone comprises (1) the Tsaté nappe, a mélange of Jurassic to Cretaceous calc-schists, metabasites, and serpentinites derived from the Piemonte–Ligurian oceanic domain (Sartori 1987), and (2) the Cimes Blanches and Frilihorn nappes which consist of successions of Permo-Mesozoic sediments with continental affinity comprising quartzites, metaarkoses, marbles, and dolomites (Caby 1981; Vannay and Allemann 1990). These sediments occur as thin dismembered sheets along the base (Cimes Blanches nappe) and structurally higher

up (Frilihorn nappe) in the Combin zone. Their origin is still debated and they have been interpreted to represent sheared-off cover sequences of the St. Bernard nappe system (e.g. Vannay and Allemann 1990), the Dent Blanche/Sesia nappe system (Pleuger et al. 2007) or to be derived from extensional allochthons within the Piemont–Ligurian oceanic domain (Dal Piaz 1999; Beltrando et al. 2014). The Combin zone reached Alpine greenschist- to blueschist-facies conditions (Reddy et al. 1999) with peak estimates around 1.2 GPa and 450 °C (Bousquet 2008) and has been interpreted as an accretionary wedge that formed at the Adriatic continental margin during Alpine subduction (Sartori 1987; Marthaler and Stampfli 1989). Rb–Sr and Ar/Ar geochronology by Reddy et al. (1999, 2003) showed that greenschist-facies deformation within the Combin zone occurred after 48 Ma, mainly between 45 and 36 Ma, but also continued afterwards as more localized deformation reworking earlier structures. The Combin zone is underlain by the Zermatt–Saas zone in the southeast and the St. Bernard nappe system in the northwest and its basal contact is the Combin Fault. The Zermatt–Saas zone is also derived from Piemont–Ligurian oceanic lithosphere and consists of Jurassic ophiolites (metabasalts, metagabbros, metaultramafics, and metasediments) which experienced high- to ultrahigh-pressure metamorphism in the Palaeocene–Eocene. U–Pb geochronology on magmatic zircons from metagabbros yielded protolith ages around 164 Ma, which are interpreted to date the age of oceanic spreading (Rubatto et al. 1998). A large spread of available (U) HP ages between ca. 62 and 40 Ma (Bowtell et al. 1994; Amato et al. 1999; Lapen et al. 2003; Mahlen et al. 2005; De Meyer et al. 2014; Skora et al. 2015; Weber et al. 2015; Fassmer et al. 2016) suggests that the Zermatt–Saas zone and associated fragments of continental crust located at high structural levels and on top of it (e.g. Ballèvre et al. 1986; Dal Piaz et al. 2001; Beltrando et al. 2010a) consist of several slivers that assembled during subduction. Peak metamorphic conditions within the Zermatt–Saas zone commonly reached 2.5–3.0 GPa and 550–600 °C (Bucher et al. 2005), while UHP metamorphism has been reported for metasediments and eclogites at Lago di Cignana in the western Valtournenche of Italy (Reinecke 1998; Groppo et al. 2009; Frezzotti et al. 2011). Peak metamorphic conditions for these rocks have been calculated at  $\geq 3.2$  GPa and  $\leq 600$  °C (Groppo et al. 2009; Frezzotti et al. 2011), and the age of metamorphism has been dated with various geochronometers. U–Pb SHRIMP dating on whole zircons and zircon rims by Rubatto et al. (1998) yielded ages of  $44.1 \pm 0.7$  Ma. Amato et al. (1999) reported a Sm–Nd garnet age of  $40.6 \pm 2.6$  Ma for a UHP eclogite, while Lapen et al. (2003) obtained a garnet–omphacite–whole-rock isochron age of  $48.8 \pm 2.1$  Ma with the Lu–Hf method for the same sample. Gouzu et al. (2006) reported an age of ca.

44–43 Ma for phengite inclusions in garnet dated with the Ar/Ar step-heating method. The Zermatt–Saas zone at Lago di Cignana partly shows a greenschist-facies overprint, which has been dated at  $38 \pm 2$  Ma by Amato et al. (1999) with Rb–Sr whole-rock–phengite chronometry. According to these ages from the Lago di Cignana area, the peak of UHP metamorphism, following prograde metamorphism around 48 Ma, probably occurred at ca. 44–43 Ma, whereas HP conditions may have lasted until ca. 41–40 Ma and greenschist-facies conditions were reached subsequently at ca. 38 Ma. The Zermatt–Saas zone is folded around the underlying Monte Rosa nappe, the palaeogeographic origin of which is still controversial. It may either be derived from the Briançonnais continental spur (e.g. Escher et al. 1997; Keller and Schmid 2001) or from the proximal European continental margin (e.g. Froitzheim 2001; Pleuger et al. 2005). In the north, the Zermatt–Saas zone dips below the Mischabel fold, a large SE-closing antiform mostly affecting continental units of the St. Bernhard nappe system, which is derived from Briançonnais continental crust (e.g. Schmid et al. 2004). The geometry of the Palaeogene nappe stack in the Swiss–Italian Western Alps has been largely modified by Oligocene–Miocene backfolding and formation of the Vanzone antiform after ca. 32 Ma (e.g. Escher et al. 1993; Keller et al. 2005 and references therein).

## Field relations and lithologies

The area around Lago di Cignana in the western Valtournenche of Italy displays a well-exposed cross section through the uppermost part of the nappe stack in the Western Alps including from top to bottom the continental Dent Blanche nappe, the composite Combin zone, and the oceanic Zermatt–Saas zone (Fig. 2a, b). The Lago di Cignana section is located on the northern limb of the regional Vanzone antiform (Fig. 1d) so that foliations mainly dip to the northwest. However, also west- and north-dipping foliations can partly be observed suggesting folding around NW–SE-trending fold axes. Ultrahigh-pressure rocks of the Zermatt–Saas zone occur south of Lago di Cignana as three dismembered slivers less than 150 m in thickness (Forster et al. 2004) and comprise coesite-bearing eclogites and quartz-rich metasediments (e.g. Reinecke 1991). They are surrounded by eclogite-facies metabasic and metasedimentary rocks which equilibrated within the quartz stability field during peak metamorphism. The (U)HP assemblage in eclogites generally consists of garnet, glaucophane, and omphacite. Retrograde minerals include hornblende, albite, epidote, and chlorite. Metasediments of the UHP slice are usually quartz-rich and consist mainly of garnet, white mica, and quartz. For detailed petrographic and petrological descriptions of UHP lithologies, the reader is referred to

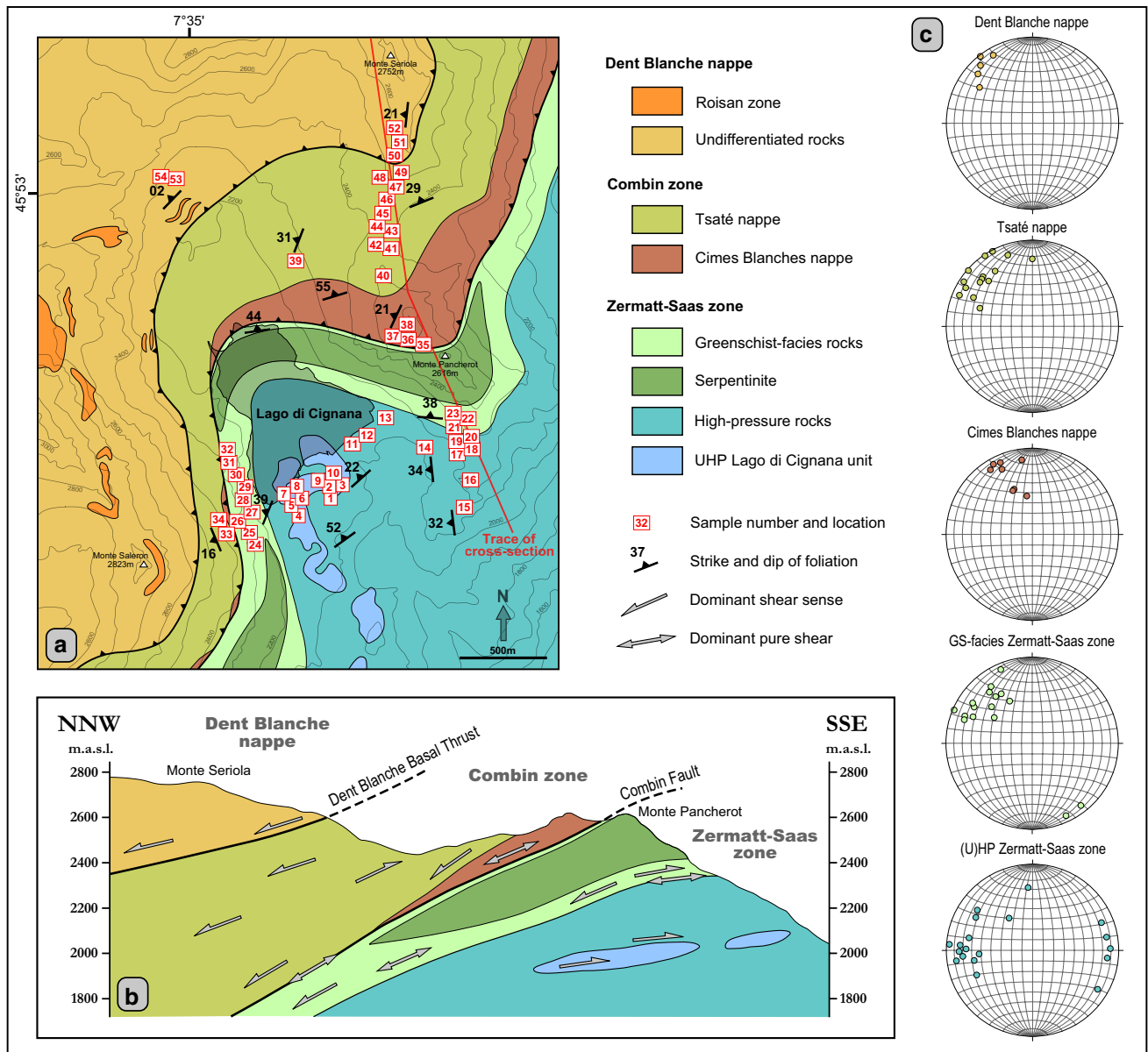


**Fig. 2** **a** Geological sketch map of the Lago di Cignana area after Tamagno (2000), Forster et al. (2004), Groppo et al. (2009), Manzotti (2011), and own observations and interpretations; locations of samples used for microstructural analyses are shown. **b** Cross section

with all units projected into the Monte Pancherot—Monte Seriola transect; shear senses are from this study. **c** Stereoplots of stretching lineations as equal area projections in the lower hemisphere

Reinecke (1998) and Groppo et al. (2009). Stretching lineations within (U)HP rocks dominantly trend E–W (Fig. 2c) but may have been rotated and reoriented during subsequent deformation phases. At higher structural levels above the UHP slice, calcschists become more abundant and may contain garnet or are garnet-free depending on the degree of retrogression. They consist of white mica, quartz, feldspar, and calcite, as well as retrograde chlorite and epidote. The uppermost part of the Zermatt–Saas zone at Lago di Cignana shows a strong greenschist-facies overprint. Metabasites are often completely retrogressed to greenschists

mainly consisting of epidote, chlorite, actinolite, and albite. Stretching lineations within strongly retrogressed calcschists and greenschists dominantly trend NW–SE (Fig. 2c). The discrimination of calcschists and greenschists of the uppermost Zermatt–Saas zone against those of the overlying Combin zone is often difficult. HP relics such as garnet within rocks at this structural level suggest affiliation with the Zermatt–Saas zone. This is supported by a difference in peak temperatures between calcschists in the footwall and hanging wall of Cimes Blancs metasediments obtained with Raman spectroscopy thermometry by Negro et al.

(2013): rocks in the footwall of the Cimes Blanches nappe record temperatures between 498 and 532 °C, whereas rocks in the hanging wall record peak temperatures of 455–475 °C. The structural position of strongly retrogressed greenschists and calcschists in the footwall of Cimes Blanches metasediments also speaks for their tectonic affiliation with the Zermatt–Saas zone (Pleuger et al. 2007; Groppo et al. 2009). Two large serpentinite bodies occur in the uppermost Zermatt–Saas zone. One builds up the ridge of Monte Pancherot east of the lake and then wedges out towards the west, the other occurs south of the lake (Fig. 2a). Metasedimentary rocks of the Cimes Blanches nappe occur at the base of the Combin zone as a large sliver north of Monte Pancherot wedging out towards the west and as small dismembered fragments southwest of the lake. The Cimes Blanches nappe comprises from bottom to top a succession of quartzites, cellular dolomites (Rauhwacke), and marbles. Quartzites also contain white mica and have a tabular appearance defined by cm- to dm-thick layers of white to greyish colour. The stretching lineation plunges to the NNW to N (Fig. 2c) and is defined by elongated quartz aggregates and aligned white mica. The Tsaté nappe builds up the main part of the Combin zone and consists mainly of calcschists with metabasite bodies and lenses. Calcschists are always garnet-free and consist of white mica, quartz, feldspar, calcite, chlorite, and epidote. Metabasites display typical greenschist-facies assemblages consisting of epidote (clinozoisite), actinolite, chlorite, and albite. Stretching lineations associated with penetrative fabrics mainly plunge to the NW (Fig. 2c). Rocks of the lowermost Dent Blanche nappe at Lago di Cignana often display greenschist-facies mylonitic fabrics and stretching lineations that plunge to the NW (Fig. 2c). A metamorphic layering consisting of alternating layers of quartz + feldspar and white mica + epidote can often be observed. Gneissic and mylonitic basement rocks are often intimately folded with slivers of the metasedimentary Roisan zone (Manzotti et al. 2014).

### Kinematic analyses and deformation structures

In this section, we describe meso- and microscopic deformation structures as well as quartz textures from the area around Lago di Cignana (Figs. 3, 4, 5, 6) to determine bulk shear senses and to gain information on the kinematics and geometry of deformation. Besides structural observations from outcrops, 54 samples were analysed in thin section (Table 1), the sample locations of which are depicted on the geological map in Fig. 2a. Shear bands, grain shape preferred orientations (GSPO), mica fish, asymmetric porphyroblasts, and occasionally the asymmetry of passive shear folds were used to determine bulk shear senses.

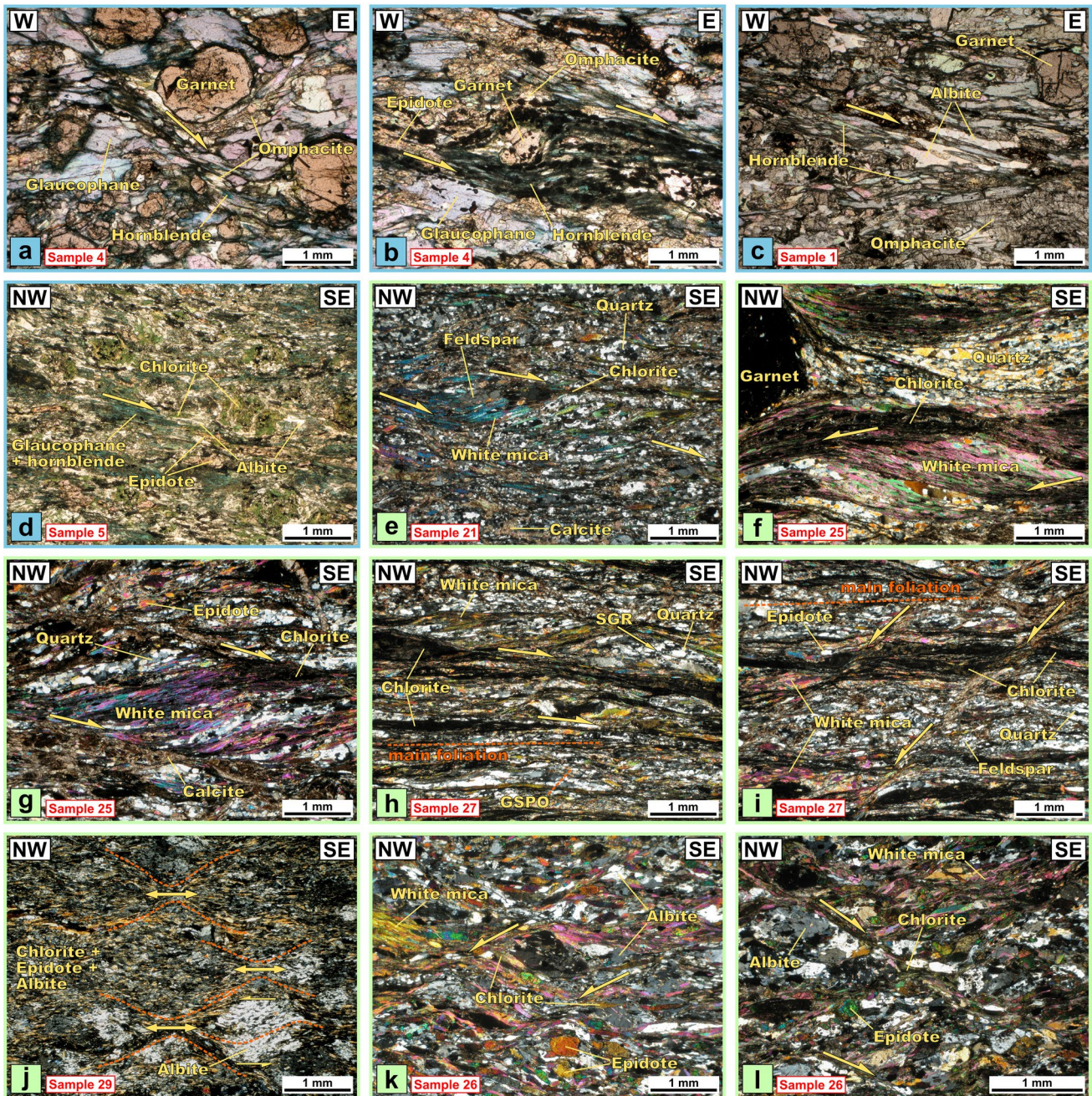
**Fig. 3** Photomicrographs of rocks from the Zermatt–Saas zone; colours of picture frames and numbering backgrounds indicate unit affiliation and correspond to the ones in Fig. 2; all thin sections were cut parallel to the xz plane of the finite strain ellipsoid. **a–d** Taken with parallel polarizers, **e–l** with crossed polarizers. **a** Sample 4: eclogite from south of Lago di Cignana showing top-E shear band with only little retrogression. **b** Same sample as before showing top-E shear bands and asymmetrically sheared hornblende between shear bands and around garnet porphyroblast suggesting deformation on the retrograde path. **c** Sample 1: eclogite from south of Lago di Cignana with hornblende and albite stable in top-E shear band indicating formation at epidote–amphibolite-facies conditions. **d** Sample 5: partly retrogressed eclogite from south of Lago di Cignana showing top-SE shear band with greenish-blue amphibole (glaucophane + hornblende), epidote, albite, and chlorite; garnet is often strongly chloritized; deformation occurred under epidote–amphibolite-facies conditions, whereas chlorite largely grew post-kinematically. **e** Sample 21: garnet-free calcschist from an outcrop south of Monte Pancherot showing top-SE shear bands. **f** Sample 25: garnet calcschist from the western side of Lago di Cignana showing retrograde top-NW shear band with chlorite stable. **g** Same sample as before showing retrograde top-SE shear band with chlorite stable. **h** Sample 27: garnet-free metasediment from southwest of the lake with shallowly dipping top-SE shear bands modifying the chlorite-bearing mylonitic foliation; a slight grain shape preferred orientation (GSPO) of quartz at the bottom of the picture indicates top-SE shearing; recrystallization of quartz by dominant subgrain rotation (SGR) suggests temperatures between 400 and 500 °C (Stipp et al. 2002). **i** Same sample as before showing steeply dipping top-NW shear bands cutting through the chlorite-bearing foliation. **j** Sample 29: fine-grained greenschist with poikiloblastic albite from the western side of Lago di Cignana showing asymmetric fabric; the internal foliation of the albite blast in the lower right corner of the picture has been slightly rotated indicating top-NW transport after main fabric formation. **k** Sample 26: greenschist from southwest of the lake showing top-NW shear bands. **l** Same sample as before showing subordinate top-SE shear bands

Microstructural analyses were made on lineation-parallel, foliation-perpendicular cuts. The relative chronology of deformation is deduced from the metamorphic grade of fabrics and deformation structures as well as overprinting and geometric relations between fabric elements and deformation structures.

### Zermatt–Saas zone

Thirty-two thin sections from different structural levels of the Zermatt–Saas zone exposed around Lago di Cignana were analysed in combination with mesoscopic deformation structures in outcrop. While the uppermost Zermatt–Saas zone shows a strong greenschist-facies overprint, pristine or only weakly retrogressed (U)HP rocks occur at lower structural levels, especially south of the lake. Accordingly, 20 thin sections were identified as fresh or weakly retrogressed (U)HP rocks and 12 as strongly overprinted at greenschist-facies conditions.

Metabasites of the UHP slice south of Lago di Cignana often display top-(S)E shear bands in thin section (samples 1, 4, and 5). Some shear bands in sample 4 display only little retrogression (Fig. 3a), most likely under retrograde,



amphibolite-facies conditions as suggested by the occurrence of hornblende (Table 2), while also stronger retrogression within strained areas as well as epidote along shear bands can be observed (Fig. 3b). In sample 1, the association of hornblende and albite within shear bands (Fig. 3c) supports the assumption that they formed on the retrograde path under low-temperature amphibolite-facies conditions. Sample 5 is a partly retrogressed eclogite in which garnet is often strongly chloritized. Glaucophane seems to be still stable within shear bands, whereas also retrogression to green amphibole, most likely hornblende, can be observed (Fig. 3d). Albite and epidote occur in

the matrix as well as along shear bands. The assemblage hornblende + albite + epidote within shear bands suggests deformation under overall epidote–amphibolite-facies conditions. Chlorite can also partly be observed along shear bands but in general seems to have largely grown post-kinematically in this sample. Top-(S)E shear bands can also often be observed in eclogite outcrops on natural cuts (sub)parallel to the lineation. Five samples were taken from metasedimentary rocks of the UHP unit. Four samples display top-E shear sense criteria, mostly sheared white mica, in thin section (samples 2, 6, 9, and 10), and one sample shows top-W kinematic indicators (sample 3).

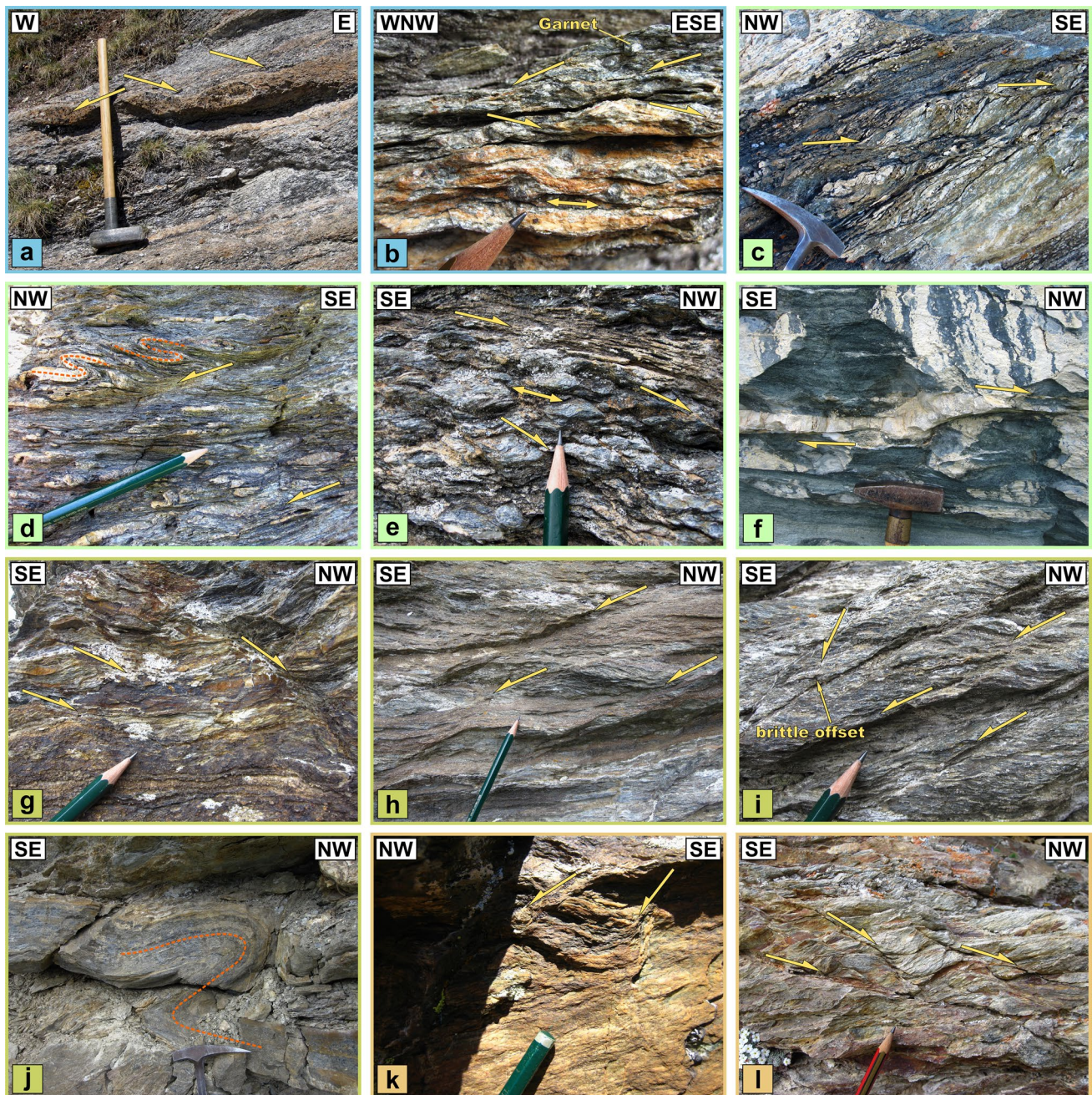


**Fig. 4** Deformation structures observed in outcrop; colours of picture frames and numbering backgrounds indicate unit affiliation and correspond to the ones in Fig. 2. **a** Metasediments of the UHP unit south of the lake showing top-E and subordinate top-W shear sense criteria associated with asymmetric boudinage of a more competent, garnet-rich layer. **b** Garnet-bearing metasediments of the Zermatt–Saas zone south of Monte Pancherot showing conjugate top-WNW and top-ESE kinematic indicators and partly a symmetric fabric. **c** Metasediments of the Zermatt–Saas zone south of Monte Pancherot displaying retrograde top-SE shear bands. **d** Top-NW shear bands within garnet-free calcschists of the Zermatt–Saas zone south of Monte Pancherot associated with rootless tight to isoclinal, intrafolial folds. **e** Calcschists of the Zermatt–Saas zone on the western side of Lago di Cignana showing top-NW shear bands, small-scale boudinage of more compe-

tent layers, and a high-strain zone in the upper part. **f** Sheared quartz layer within greenschists of the Zermatt–Saas zone west of Lago di Cignana indicating a top-NW shear sense. **g** Top-NW shear bands within calcschists of the Combin zone west of Lago di Cignana. **h** Tight NW-vergent fold within Combin metasediments southwest of Lago di Cignana; asymmetry suggests top-NW transport. **i** Top-SE shear bands within calcschists at the base of the Combin zone on the eastern slope of Monte Saleron. **j** Top-SE shear bands within calcschists at the base of the Combin zone on the eastern slope of Monte Saleron; more steeply dipping top-SE shear planes brittily offsetting the foliation can also be observed. **k** Ductile top-NW shear bands within Dent Blanche gneisses south of Monte Seriola. **l** Ductile to semi-ductile top-NW shear bands within Dent Blanche gneisses north of Lago di Cignana

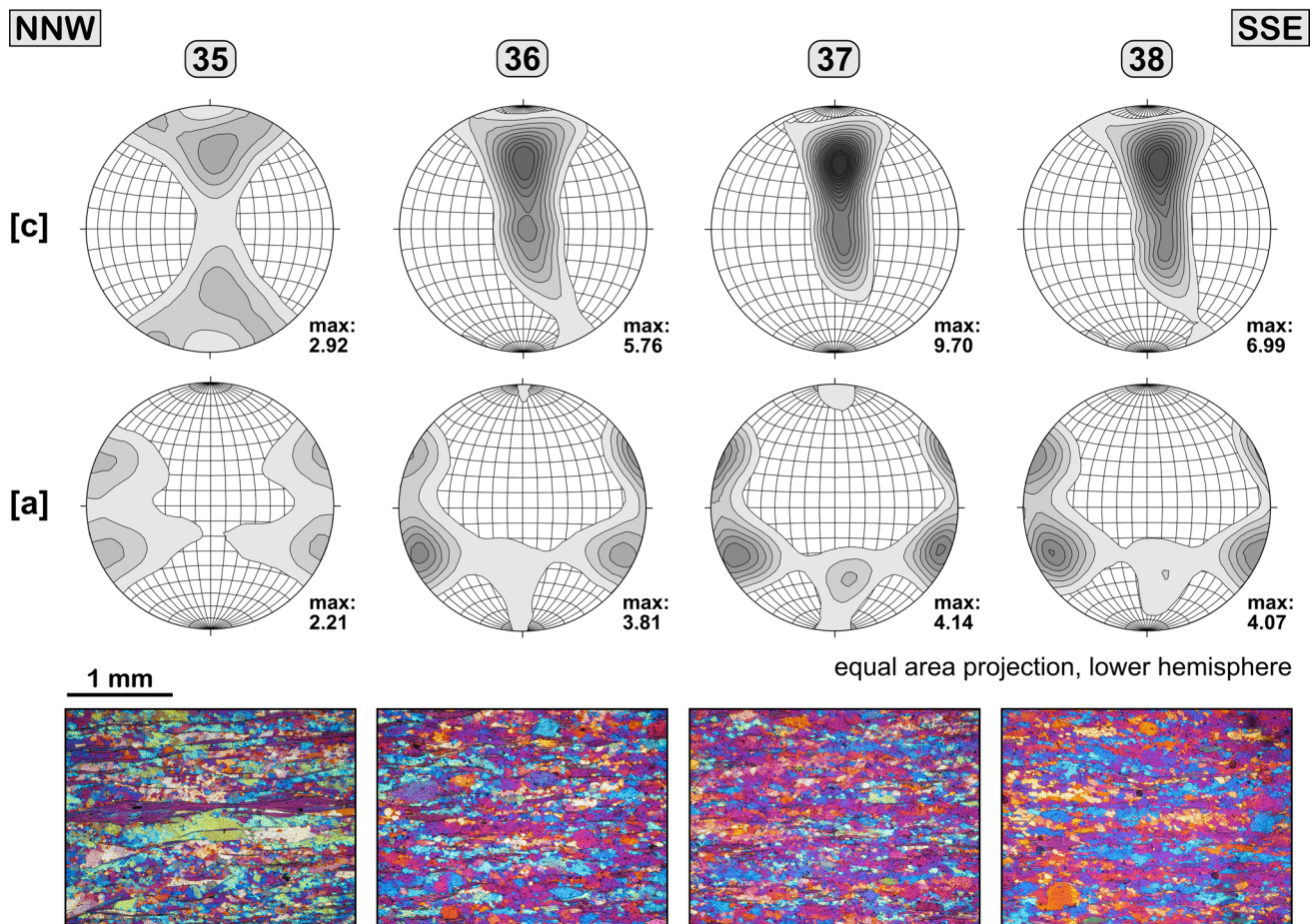


**Fig. 5** Pole figures of [c]- and [a]-axes distributions of quartzites from the Cimes Blancs nappe at the base of the Combin zone; equal area projections in the lower hemisphere; maxima of isolines being multiples of random distribution are indicated; the xy plane in pole figures corresponds to the foliation and the x-direction to the stretching lineation measured in the field; pole figures are orthorhombic and indicate dominant coaxial deformation under greenschist-facies conditions (see text for further discussion); c-axis opening angles around  $50^\circ$  suggest temperatures of  $ca. 400 \pm 50^\circ C$  during texture formation (Kruhl 1996; Law et al. 2004); photomicrographs at the bottom correspond to the samples labelled above and were taken with gypsum plate inserted

samples were collected along the ridge south of Monte Pancherot across the transition between well-preserved HP rocks in the footwall and pervasively retrogressed rocks in the hanging wall (samples 17–23). Three of these show kinematic indicators indicating top-S(E) shearing (samples 19, 21, and 23), 3 of them display kinematic indicators indicating top-(N)W shearing (samples 17, 18, and 20), and one sample shows ambiguous shear sense criteria in thin section (sample 22). Conjugate top-(N)W and top-(S)E kinematic indicators can also sometimes be observed in outcrop. Some garnet-bearing metasediments south of Monte Pancherot show conjugate sets of shear bands as well as symmetric flexure of the foliation (Fig. 4b). Two samples from this locality show top-(N)W kinematic indicators in thin section (samples 17 and 18). Above these metasediments, a m-thick layer of serpentinite separates the metasediments in the footwall from a layer of metabasites in the

The metamorphic grade of the deformation structures in these metasediments is difficult to determine due to the lack of diagnostic minerals. In an outcrop in the eastern part of the UHP slice, more competent garnet-rich layers within quartz-rich metasedimentary material are boudinaged and dismembered into lenses and nodules. Top-E kinematic indicators, mostly shear bands and asymmetric porphyroblasts, are abundant in the host material, whereas rare and more discrete top-W shear bands truncate garnet-rich layers (Fig. 4a). Two samples were taken from partly isoclinally folded quartz veins from the western part of the UHP slice (samples 7 and 8). Sample 8 displays a slight grain shape preferred orientation, which suggests top-NW shearing, whereas sample 7 does not give any kinematic indicators. Six eclogite samples were collected from outcrops southeast of Lago di Cignana but did not yield any shear sense criteria (samples 11–16). Seven metasediments

samples were collected along the ridge south of Monte Pancherot across the transition between well-preserved HP rocks in the footwall and pervasively retrogressed rocks in the hanging wall (samples 17–23). Three of these show kinematic indicators indicating top-S(E) shearing (samples 19, 21, and 23), 3 of them display kinematic indicators indicating top-(N)W shearing (samples 17, 18, and 20), and one sample shows ambiguous shear sense criteria in thin section (sample 22). Conjugate top-(N)W and top-(S)E kinematic indicators can also sometimes be observed in outcrop. Some garnet-bearing metasediments south of Monte Pancherot show conjugate sets of shear bands as well as symmetric flexure of the foliation (Fig. 4b). Two samples from this locality show top-(N)W kinematic indicators in thin section (samples 17 and 18). Above these metasediments, a m-thick layer of serpentinite separates the metasediments in the footwall from a layer of metabasites in the



hanging wall. Serpentinite layers and layer-parallel quartz veins are necked and boudinaged symmetrically suggesting dominant coaxial deformation without a significant rotational component. Further into the hanging wall, metasediments are cut by shallowly dipping, garnet-free top-SE shear bands overprinting an older layer-parallel foliation (Fig. 4c). Two samples taken close to this outcrop, a partly retrogressed garnet-bearing metasediment (sample 19) and a garnet-free calcschist (sample 21), display greenschist-facies top-S shear bands in thin section (Fig. 3e). Further into the hanging wall, strongly retrogressed calcschists show top-NW kinematic indicators in outcrop (Fig. 4d).

Top-NW shear bands are often associated with rootless tight to isoclinal, intrafolial passive shear folds. A garnet-free calcschist sample taken from an outcrop in the hanging wall (sample 23), however, shows retrograde, i.e. greenschist-facies shear bands indicating top-SE shearing.

Pervasively retrogressed rocks of the uppermost Zermatt–Saas zone are also well-exposed on the western side of Lago di Cignana where 9 samples were taken for thin-section analyses. All kinematic indicators observed in this area formed under greenschist-facies conditions as is evident from the presence of syn-kinematic greenschist-facies mineral assemblages. Two samples exhibit top-NW

◀ **Fig. 6** Photomicrographs of rocks from the Combin zone and the Dent Blanche nappe; *colours of picture frames and numbering backgrounds* indicate unit affiliation and correspond to the ones in Fig. 2; all thin sections were cut parallel to the xz plane of the finite strain ellipsoid and all pictures were taken with crossed polarizers. **a** Sample 35: quartzite from the Cimes Blanches nappe northwest of Monte Pancherot with necked white mica indicating coaxial deformation; a slight grain shape preferred orientation (GSPO) indicates a top-SSE shear sense and recrystallization of quartz by dominant subgrain rotation (SGR) suggests temperatures during deformation between ca. 400 and 500 °C (Stipp et al. 2002). **b** Same sample as before showing top-SSE and top-NNW shear bands as well as a slight GSPO indicating a top-NNW shear sense; recrystallization of quartz by dominant SGR again suggests temperatures between ca. 400 and 500 °C. **c** Sample 40: calcschist from the lower Tsaté nappe northwest of Monte Pancherot displaying a metamorphic layering consisting of white mica + chlorite and quartz + calcite + feldspar; discrete top-NNW shear bands overprint the foliation and are associated with brittle fracturing and dismembering of feldspar suggesting temperatures below 450 °C (e.g. Pryer, 1993). **d** Same sample as before showing semi-ductile top-NNW shear band truncating the foliation. **e** Sample 43: greenschist from the crest south of Monte Seriola displaying top-SSE shear band. **f** Sample 52: quartz-rich mylonite from the lowermost Dent Blanche nappe south of Monte Seriola; a quartz GSPO and the vergence of the asymmetric fold indicate top-NW transport; recrystallization of quartz probably occurred by dominant SGR suggesting temperatures during deformation between ca. 400 and 500 °C (Stipp et al. 2002). **g** Sample 51: mylonite from the lowermost Dent Blanche nappe south of Monte Seriola; the greenschist-facies metamorphic layering is folded into isoclinal recumbent folds which are truncated by a late semi-ductile top-NW shear band. **h** Same sample as before displaying discrete semi-ductile top-NW shear bands truncating the foliation. **i** Same sample as before showing steeply dipping brittle top-SE shear planes. **j** Sample 54: gneiss from the lower Dent Blanche nappe northwest of Lago di Cignana showing top-NW shear band and associated undulose and patchy extinction of quartz suggesting lower greenschist-facies conditions probably between 280 and 400 °C during deformation (Stipp et al. 2002); grain boundary migration (GBM) of quartz at the bottom of the picture probably represents a pre-Alpine relic. **k** Same sample as before showing undulose/patchy extinction of large quartz grains and partly bulging recrystallization (BLG) suggesting temperatures between 280 and 400 °C during deformation (Stipp et al. 2002). **l** Sample 53: gneiss from the same outcrop as before with folded quartz layers which are cut by brittle top-NNW shear planes suggesting deformation at temperatures below ca. 280 °C (Stipp et al. 2002)

kinematic indicators (samples 24 and 26), and 7 samples display symmetric fabrics and conjugate sets of top-NW/top-SE shear bands (samples 25, 27, and 28–32). Relic garnet can often be observed within strongly retrogressed metagabbroic rocks and calcschists. A garnet micaschist (sample 25) from this domain shows shear bands indicating top-NW as well as top-SE shearing (Fig. 3f, g). Chlorite replaces white mica in sheared domains documenting the greenschist-facies grade of this deformation. A garnet-bearing calcschist from a nearby outcrop displays dominant top-NW shear bands (sample 24). Further to the north and into the hanging wall, calcschists become progressively more retrogressed so that garnet is not preserved anymore. A calcschist from this domain (sample 27) shows conjugate

sets of shear bands. Chlorite occurs as large grains as part of the mylonitic foliation, which has later been modified by shear band formation so that chlorite is often transected and offset by these shear bands. Top-SE shear bands often dip very shallowly with respect to the mylonitic foliation (Fig. 3h), while top-NW shear bands truncate the foliation at a relatively high angle (Fig. 3i). These geometric relations suggest that coaxial deformation postdates initial greenschist-facies retrogression and fabric formation. Quartz ribbons sometimes show slight GSPOs indicating SE-vergent shearing and quartz seems to have dominantly recrystallized by subgrain rotation (SGR; Fig. 3h) suggesting temperatures between ca. 400 and 500 °C (Stipp et al. 2002). Calcschists southwest of the lake often display mesoscopic top-NW shear bands in outcrop, which are often associated with small-scale boudinage of more competent layers suggesting a pure shear component during bulk top-NW shearing (Fig. 4e). Further to the north, greenschists just below the Combin Fault (samples 28–32) show symmetric fabrics in thin section (Fig. 3j). Albite blasts are poikiloblastic and inclusions consist of the matrix phases. They are aligned with the main foliation, suggesting that they grew syn-kinematically during greenschist-facies retrogression. Poikiloblastic albite has sometimes been slightly rotated as suggested by flexure of the internal foliation (Fig. 3j). A greenschist from a nearby outcrop (sample 26) mainly displays top-NW shear bands in thin section (Fig. 3k) but also partly top-SE shear bands (Fig. 3l) as well as symmetric fabric domains. In outcrop, sheared quartz layers within these greenschists also occasionally indicate top-NW shearing (Fig. 4f).

In summary, rocks of the Zermatt–Saas zone at Lago di Cignana show complex kinematic indicators through the different structural levels from pristine and weakly retrogressed (U)HP rocks in the footwall to strongly retrogressed, greenschist-facies rocks of the uppermost part. No clear kinematic indicators could be observed within eclogites adjacent to the UHP unit. Eclogites from the UHP slice, on the other hand, display epidote–amphibolite-facies, and possibly some higher-pressure top-(S)E shear sense criteria, that can be attributed to deformation on the retrograde path. Also, UHP metasediments show mainly top-(ES)E kinematic indicators which, however, cannot be unambiguously attributed to metamorphic conditions during deformation. While top-(S)E kinematic indicators dominate within UHP rocks, strongly retrogressed rocks at higher structural levels towards the Combin Fault are characterized by alternating zones of dominant top-SE and top-NW shear, respectively, as well as conjugate top-SE/NW kinematic indicators and symmetric fabrics indicating dominant pure shear deformation along this structural domain.

**Table 1** Table of samples taken for thin-section analyses with values for dip directions and angles of foliations, plunge directions and angles of stretching lineations, shear senses and metamorphic grade of kinematic indicators: HP = high-pressure conditions, EA = epidote–amphibolite-facies conditions, GS = greenschist-facies conditions

| No. | Unit           | Lithology      | Foliation | Lineation | Shear sense | Grade |
|-----|----------------|----------------|-----------|-----------|-------------|-------|
| 54  | Dent Blanche   | Gneiss         | 314/02    | 322/02    | Top-NW      | GS    |
| 53  | Dent Blanche   | Gneiss         | 288/12    | 330/10    | Top-NNW     | GS    |
| 52  | Dent Blanche   | Gneiss         | 276/21    | 318/11    | Top-NW      | GS    |
| 51  | Dent Blanche   | Gneiss         | 244/22    | 312/16    | Top-NW      | GS    |
| 50  | Dent Blanche   | Gneiss         | 254/35    | 304/27    | Top-NW      | GS    |
| 49  | Tsaté          | Calcschist     | 296/29    | 311/02    | Conjugate   | GS    |
| 48  | Tsaté          | Calcschist     | 296/09    | 293/09    | Top-WNW     | GS    |
| 47  | Tsaté          | Calcschist     | 274/27    | 313/21    | Top-NW      | GS    |
| 46  | Tsaté          | Greenschist    | 342/24    | 300/12    | Top-WNW     | GS    |
| 45  | Tsaté          | Calcschist     | 322/21    | 00/23     | Top-S       | GS    |
| 44  | Tsaté          | Greenschist    | 338/29    | 296/25    | Top-WNW     | GS    |
| 43  | Tsaté          | Greenschist    | 66/15     | 332/02    | Top-SSE     | GS    |
| 42  | Tsaté          | Greenschist    | 08/08     | 303/06    | Top-WNW     | GS    |
| 41  | Tsaté          | Greenschist    | 325/20    | 315/20    | Top-NW      | GS    |
| 40  | Tsaté          | Calcschist     | 288/24    | 341/14    | Top-NNW     | GS    |
| 39  | Tsaté          | Calcschist     | 291/31    | 316/28    | Top-NW      | GS    |
| 38  | Cimes Blanches | Quartzite      | 278/20    | 327/12    | Top-NNW     | GS    |
| 37  | Cimes Blanches | Quartzite      | 295/21    | 335/18    | Top-NNW     | GS    |
| 36  | Cimes Blanches | Quartzite      | 269/10    | 331/08    | Top-NNW     | GS    |
| 35  | Cimes Blanches | Quartzite      | 319/10    | 336/10    | Conjugate   | GS    |
| 34  | Tsaté          | Calcschist     | 247/16    | 199/11    | Conjugate   | GS    |
| 33  | Tsaté          | Calcschist     | 248/10    | 326/02    | Top-NW      | GS    |
| 32  | Zermatt–Saas   | Greenschist    | 81/13     | 89/11     | Conjugate   | GS    |
| 31  | Zermatt–Saas   | Greenschist    | 64/16     | 68/15     | Conjugate   | GS    |
| 30  | Zermatt–Saas   | Greenschist    | 244/04    | 293/02    | Conjugate   | GS    |
| 29  | Zermatt–Saas   | Greenschist    | 208/32    | 142/09    | Conjugate   | GS    |
| 28  | Zermatt–Saas   | Greenschist    | 217/12    | 155/08    | Conjugate   | GS    |
| 27  | Zermatt–Saas   | Calcschist     | 92/39     | 328/33    | Conjugate   | GS    |
| 26  | Zermatt–Saas   | Greenschist    | 306/35    | 322/32    | Top-NW      | GS    |
| 25  | Zermatt–Saas   | Grt calcschist | 318/44    | 332/44    | Conjugate   | GS    |
| 24  | Zermatt–Saas   | Grt calcschist | 323/50    | 304/46    | Top-NW      | GS    |
| 23  | Zermatt–Saas   | Calcschist     | 337/28    | 320/24    | Top-SE      | GS    |
| 22  | Zermatt–Saas   | Calcschist     | 356/31    | 304/18    | Conjugate   | GS    |
| 21  | Zermatt–Saas   | Calcschist     | 350/35    | 356/28    | Top-S       | GS    |
| 20  | Zermatt–Saas   | Metasediment   | 313/27    | 300/25    | Top-NW      | GS    |
| 19  | Zermatt–Saas   | Metasediment   | 02/32     | 274/04    | Top-S       | GS    |
| 18  | Zermatt–Saas   | Metasediment   | 04/29     | 294/26    | Top-W       | HP    |
| 17  | Zermatt–Saas   | Metasediment   | 04/38     | 302/22    | Top-NW      | GS    |
| 16  | Zermatt–Saas   | Eclogite       | 188/39    | 262/12    | –           | –     |
| 15  | Zermatt–Saas   | Eclogite       | 263/32    | 246/30    | –           | –     |
| 14  | Zermatt–Saas   | Eclogite       | 264/34    | 306/22    | –           | –     |
| 13  | Zermatt–Saas   | Eclogite       | 284/31    | 271/24    | –           | –     |
| 12  | Zermatt–Saas   | Eclogite       | 319/40    | 265/20    | –           | –     |
| 11  | Zermatt–Saas   | Eclogite       | 274/33    | 260/21    | –           | –     |
| 10  | Zermatt–Saas   | Metasediment   | 68/17     | 96/14     | Top-E       | HP?   |
| 9   | Zermatt–Saas   | Metasediment   | 163/48    | 80/14     | Top-E       | GS?   |
| 8   | Zermatt–Saas   | Quartzite      | 315/19    | 292/17    | Top-WNW     | GS    |
| 7   | Zermatt–Saas   | Quartzite      | 256/23    | 289/18    | –           | –     |
| 6   | Zermatt–Saas   | Metasediment   | 69/13     | 121/13    | Top-ESE     | HP?   |
| 5   | Zermatt–Saas   | Eclogite       | 324/52    | 324/52    | Top-SE      | EA    |

**Table 1** continued

| No. | Unit         | Lithology    | Foliation | Lineation | Shear sense | Grade |
|-----|--------------|--------------|-----------|-----------|-------------|-------|
| 4   | Zermatt–Saas | Eclogite     | 318/22    | 269/16    | Top-E       | EA    |
| 3   | Zermatt–Saas | Metasediment | 297/39    | 266/38    | Top-W       | HP?   |
| 2   | Zermatt–Saas | Metasediment | 344/37    | 281/26    | Top-E       | HP?   |
| 1   | Zermatt–Saas | Eclogite     | 334/29    | 274/17    | Top-E       | EA    |

**Table 2** Electron microprobe analyses of retrograde minerals within samples from the Zermatt–Saas and Combin zones; mineral compositions were measured with the Jeol JXA-8200 superprobe at the Steinmann-Institut of the University of Bonn; note the different compositions of amphiboles within the two samples: retrograde amphibole in sample 4, a partly retrogressed eclogite from the Zermatt–Saas zone, is hornblende suggesting formation at epidote–amphibolite-facies conditions together with albite and epidote, while amphibole in sample 43, a greenschist from the Combin zone, is actinolite suggesting formation at greenschist-facies conditions

|                                | Sample 4: Zermatt–Saas eclogite |       |       |       |        | Sample 43: Combin greenschist |       |       |       |       |       |       |        |
|--------------------------------|---------------------------------|-------|-------|-------|--------|-------------------------------|-------|-------|-------|-------|-------|-------|--------|
|                                | Amp                             | Amp   | Ep    | Czo   | Ab     | Amp                           | Amp   | Chl   | Chl   | Phg   | Phg   | Czo   | Ab     |
| SiO <sub>2</sub>               | 48.40                           | 47.24 | 38.17 | 39.03 | 67.68  | 56.13                         | 56.51 | 28.74 | 28.07 | 53.02 | 52.50 | 39.47 | 68.44  |
| Al <sub>2</sub> O <sub>3</sub> | 10.41                           | 11.48 | 28.38 | 32.13 | 20.21  | 1.34                          | 0.92  | 19.94 | 21.57 | 26.71 | 27.48 | 32.36 | 19.79  |
| MgO                            | 12.34                           | 12.10 | 0.06  | 0.05  | 0.12   | 20.21                         | 20.78 | 26.87 | 26.06 | 4.15  | 3.94  | 0.00  | 0.00   |
| FeO <sup>a</sup>               | 12.83                           | 13.32 | 6.38  | 1.79  | 0.28   | 5.66                          | 5.01  | 9.97  | 9.78  | 1.29  | 1.07  | 0.88  | 0.03   |
| MnO                            | 0.14                            | 0.28  | 0.08  | 0.00  | 0.07   | 0.25                          | 0.18  | 0.19  | 0.19  | 0.07  | 0.00  | 0.00  | 0.01   |
| CaO                            | 8.64                            | 8.88  | 24.01 | 24.52 | 0.59   | 12.20                         | 12.87 | 0.00  | 0.04  | 0.00  | 0.04  | 25.31 | 0.04   |
| Na <sub>2</sub> O              | 3.61                            | 3.56  | 0.00  | 0.04  | 11.01  | 0.66                          | 0.40  | 0.02  | 0.02  | 0.15  | 0.17  | 0.00  | 11.72  |
| K <sub>2</sub> O               | 0.26                            | 0.31  | 0.00  | 0.00  | 0.06   | 0.08                          | 0.03  | 0.00  | 0.00  | 10.70 | 11.11 | 0.01  | 0.06   |
| TiO <sub>2</sub>               | 0.21                            | 0.07  | 0.10  | 0.07  | 0.04   | 0.01                          | 0.02  | 0.04  | 0.02  | 0.10  | 0.14  | 0.06  | 0.00   |
| Cr <sub>2</sub> O <sub>3</sub> | 0.03                            | 0.00  | 0.04  | 0.04  | 0.00   | 0.00                          | 0.04  | 0.15  | 0.04  | 0.76  | 0.94  | 0.19  | 0.02   |
| Total                          | 96.85                           | 97.23 | 97.22 | 97.66 | 100.06 | 96.53                         | 96.77 | 85.93 | 85.79 | 96.93 | 97.38 | 98.28 | 100.10 |
| Si                             | 7.06                            | 6.90  | 2.90  | 2.88  | 2.96   | 7.90                          | 7.91  | 5.68  | 5.55  | 6.92  | 6.84  | 2.88  | 2.99   |
| Al                             | 1.79                            | 1.98  | 2.54  | 2.79  | 1.04   | 0.22                          | 0.15  | 4.65  | 5.03  | 4.11  | 4.22  | 2.79  | 1.02   |
| Mg                             | 2.68                            | 2.64  | 0.01  | 0.00  | 0.01   | 4.24                          | 4.34  | 7.92  | 7.68  | 0.81  | 0.76  | 0.00  | 0.00   |
| Fe                             | 1.56                            | 1.63  | 0.41  | 0.11  | 0.01   | 0.67                          | 0.59  | 1.65  | 1.62  | 0.14  | 0.12  | 0.05  | 0.00   |
| Mn                             | 0.02                            | 0.03  | 0.01  | 0.00  | 0.00   | 0.03                          | 0.02  | 0.03  | 0.03  | 0.01  | 0.00  | 0.00  | 0.00   |
| Ca                             | 1.35                            | 1.39  | 1.95  | 1.94  | 0.03   | 1.84                          | 1.93  | 0.00  | 0.01  | 0.00  | 0.01  | 1.98  | 0.00   |
| Na                             | 1.02                            | 1.01  | 0.00  | 0.01  | 0.93   | 0.18                          | 0.11  | 0.01  | 0.01  | 0.04  | 0.04  | 0.00  | 0.99   |
| K                              | 0.05                            | 0.06  | 0.00  | 0.00  | 0.00   | 0.01                          | 0.01  | 0.00  | 0.00  | 1.78  | 1.85  | 0.00  | 0.00   |
| Ti                             | 0.02                            | 0.01  | 0.01  | 0.00  | 0.00   | 0.00                          | 0.00  | 0.01  | 0.00  | 0.01  | 0.01  | 0.00  | 0.00   |
| Cr                             | 0.00                            | 0.00  | 0.00  | 0.00  | 0.00   | 0.00                          | 0.00  | 0.02  | 0.01  | 0.08  | 0.10  | 0.01  | 0.00   |
| Total                          | 15.56                           | 15.63 | 7.82  | 7.73  | 4.99   | 15.09                         | 15.06 | 19.98 | 19.93 | 13.89 | 13.94 | 7.72  | 5.00   |

<sup>a</sup> All iron was measured as Fe<sup>2+</sup>

## Combin zone

### *Cimes Blanches nappe*

Quartzites close to the base of the Cimes Blanches nappe and the Combin zone, respectively, were used for microstructural and textural analyses (Fig. 5) to gain information on the kinematics and geometry of deformation in the direct hanging wall of the Combin Fault. Four samples (samples 35–38) were taken from outcrops several metres in the hanging wall of the Combin Fault with sample 35 being the one closest to the contact and sample 38 the one farthest away. Samples 36–38 are mineralogically and texturally very similar. They consist of quartz with only minor amounts of white mica and feldspar. They are mostly equigranular, have a medium grain size, and only show slight

textural domains (Fig. 5). Rare shear bands and mica fish indicate top-NNW transport. Sample 35 contains more white mica and locally shows textural domains with larger quartz grains showing subgrain formation. Slight GSPOs in different domains suggest top-SSE (Fig. 6a) as well as top-NNW (Fig. 6b) shearing, and also shear bands are often conjugate (Fig. 6a, b). Recrystallization of quartz by dominant SGR (Fig. 6a, b) suggests temperatures between ca. 400 and 500 °C during fabric formation (Stipp et al. 2002).

Textures of the four quartzites were measured with the X-ray texture goniometer at Geowissenschaftliches Zentrum Universität Göttingen. Figure 5 depicts pole figures for [c]- and [a]-axes as equal area projections in the lower hemisphere with isolines being multiples of random distribution. The xy plane in the pole figures corresponds to the foliation measured in the field, and the x-direction

corresponds to the measured stretching lineation. All four samples show cross-girdle type [c]-axis pole figures as a basis (e.g. Schmid and Casey 1986). Rhomb <a> slip is dominant in all samples. Different contributions of basal <a> and prism <a> slip modify the basic cross-girdles into partial cross-girdles. The activity of these different slip systems and the absence of a single basal <a> maximum around the y-axis suggest texture formation at temperatures below 500 °C (Stipp et al. 2002). C-axis opening angles in the pole figures are consistently around 50° suggesting temperatures of ca. 400 ± 50 °C during texture formation (Kruhl 1996; Law et al. 2004). [a]-axes form small circles about 25° away from the x-direction. [c]- and [a]-axes distributions have orthorhombic symmetries suggesting dominant coaxial deformation. The different intensities of the textures are probably an effect of strain localization with sample 37 representing a zone of relatively high strain and sample 35 a zone of relatively low strain during overall pure shear deformation. The higher content of white mica in sample 35 may have also contributed to the lower intensities measured for this sample.

Microstructural and textural analyses on Cimes Blanches quartzites suggest that the base of the Combin zone at Lago di Cignana experienced dominant coaxial deformation. The measured textures show overall orthorhombic symmetries suggesting no significant rotational component. Dominant pure shear deformation is also suggested by conjugate top-NNW and top-SSE shear bands as well as domains with NNW- and SSE-vergent GSPOs in sample 35. Considering temperature estimates according to c-axis opening angles in pole figures and observed SGR in thin section, conditions during this phase were probably between ca. 400 and 450 °C. Top-NNW kinematic indicators in samples 36–38 may reflect a late top-NNW overprint following the phase of dominant pure shear deformation.

#### *Tsaté nappe*

Thirteen samples were taken from the Tsaté nappe for thin-section analyses, most of them along the crest northeast of Lago di Cignana between Monte Pancherot in the south and Monte Seriola in the north. Most samples from the crest show top-WNW to top-NNW kinematic indicators in thin section (samples 40–42, 44, 46–48), and only two samples display top-SSE to top-S kinematic indicators (samples 43 and 45). In a fine-grained greenschist from the lower Tsaté nappe, strain has been localized into top-NW shear bands (sample 41). The matrix and inclusion trails of poikiloblastic albite blasts sometimes show a sigmoidal shape suggesting syn-kinematic growth of greenschist-facies minerals during top-NW shearing. Calcschists often show a strong metamorphic layering defined by ribbons and layers of quartz + calcite and white mica + chlorite (e.g. sample 40;

Fig. 6c, d). Chlorite often occurs as large grains as part of the foliation, suggesting that the main phase of fabric formation occurred during greenschist-facies retrogression. Discrete ductile to semi-ductile top-NNW shear bands often truncating and overprinting the foliation (Fig. 6c, d) suggest top-NNW shearing under lower-grade greenschist-facies conditions. Feldspar clasts are often brittly fractured adjacent to these shear bands (Fig. 6c) suggesting temperatures below ca. 450 °C during deformation (e.g. Pryer 1993). Top-S(SE) kinematic indicators can be observed in two samples from the central part of the Tsaté nappe. In a greenschist (sample 43), actinolite and clinozoisite are stable within shear bands (Fig. 6e) suggesting formation under greenschist-facies conditions (see also Table 2). Southwest of Lago di Cignana, foliations within schists dip shallowly to the WSW. There, top-NW as well as top-SE shear bands can be observed in the direct hanging wall of the Combin Fault. Top-NW shear bands dip shallowly to moderately to the northwest (Fig. 4g), while top-SE shear bands dip shallowly to the southeast (Fig. 4h). No overprinting relations could be observed between these spatially associated but opposing kinematic indicators. Two calcschist samples from this locality show top-NW (sample 33) and conjugate (sample 34) kinematic indicators, respectively, in thin section. In outcrop, steeply dipping top-SE shear planes can be observed to overprint the ductile fabric in a brittle manner (Fig. 4i). Tight folds occur within heterogeneous metasediments just above the Combin Fault (Fig. 4j). Their asymmetry suggests NW-vergent shearing.

In summary, the Tsaté nappe at Lago di Cignana experienced bulk top-NW shearing under greenschist-facies conditions. Nine of 13 samples show top-WNW to NNW shear sense criteria, 2 show top-(S)SE kinematic indicators, and 2 thin sections display symmetric fabrics. While top-NW shearing was dominant at higher structural levels, meso- and microstructures in the direct hanging wall of the Combin Fault southwest of the lake also indicate conjugate top-NW and top-SE shearing and therefore a significant pure shear component. In some samples, top-NW shear bands seem to be related to the main phase of greenschist-facies retrogression and fabric formation, whereas in others, top-NW shear bands appear to be a late feature of renewed top-NW shearing. Top-SE to top-S shear sense criteria within rocks from the central part of the Tsaté nappe and in the hanging wall of the Combin Fault may be kinematically related and may represent conjugate shear zones to predominantly observed zones of top-NW shear.

#### **Dent Blanche nappe**

Greenschist-facies foliations within rocks of the lowest Dent Blanche nappe have often been modified and overprinted by subsequent deformation after initial

greenschist-facies retrogression and fabric formation. South of Monte Seriola, ductile top-NW shear bands can be observed in outcrop within gneisses of the lowermost Dent Blanche nappe (Fig. 4k). Three samples from this locality were analysed in thin section (samples 50–52). Quartz-rich mylonites show GSPOs of quartz grains indicating top-NW transport (samples 50 and 52; Fig. 6f). Dynamic recrystallization of quartz probably occurred mainly by SGR (Fig. 6f) indicating temperatures between ca. 400 and 500 °C (Stipp et al. 2002). Quartz layers defined by different grain sizes are sometimes folded into tight to isoclinal, NW-vergent folds and the quartz GSPO defines a NW-vergent axial surface foliation indicating folding during progressive top-NW deformation (Fig. 6f). In a sample showing a pronounced greenschist-facies metamorphic layering (sample 51), quartz ribbons sometimes show GSPOs, again indicating top-NW shearing. The foliation has been affected by isoclinal, recumbent folding (Fig. 6g), most likely during progressive deformation after initial fabric formation. Folds and the foliation in turn are truncated by shallowly to moderately dipping, semi-ductile to brittle top-NW shear bands and planes, respectively (Fig. 6g, h). These probably formed during a relatively late stage of NW-vergent shearing. In the same sample, the foliation is also cut by brittle, moderately to steeply dipping top-SE microfaults which represent late structures after cessation of ductile deformation within these rocks (Fig. 6i). Gneisses and mylonites cropping out along the plains north of Lago di Cignana also show deformation structures related to top-NW shearing. Shear bands observed in outcrop are often discrete and have a ductile to semi-ductile character (Fig. 4l). In thin section, top-NW shear bands are often localized within domains of fine-grained intergrowths of white mica + epidote + chlorite, which are often associated with large quartz grains showing patchy and undulose extinction (sample 54; Fig. 6j). In the same sample, quartz also shows dynamic recrystallization by bulging (Fig. 6k) indicating temperatures between ca. 280 and 400 °C (Stipp et al. 2002). Rare recrystallization of quartz by grain boundary migration (GBM) indicates temperatures above ca. 500 °C and is therefore interpreted to be a relic from a preceding stage of Alpine or pre-Alpine higher-grade deformation before the onset of Alpine greenschist-facies deformation along the DBBT. In sample 53, the foliation defined by quartz ribbons in a matrix of white mica + epidote + chlorite has been folded into recumbent, open to tight folds which are cut by discrete top-NNW microfaults (Fig. 6l) indicating continuing deformation in the brittle regime.

In summary, the lowermost Dent Blanche nappe at Lago di Cignana exhibits deformation structures indicating episodic or prolonged top-NW shearing under decreasing greenschist-facies conditions including initial formation of greenschist-facies fabrics, folding of foliations during

progressive deformation, and formation of semi-ductile to brittle shear bands and planes, respectively.

## Discussion

### Kinematic evolution of shear zones

Shear zones and deformation structures exposed in the area around Lago di Cignana are characterized by different bulk shear senses and metamorphic grades as well as varying amounts of rotational and coaxial deformation. Eclogites and metasediments of the UHP unit south of the lake mainly record top-(S)E kinematic indicators. Although their metamorphic grade is often not trivial to deduce from petrographic and microstructural observations, UHP eclogites display deformation structures and mineral assemblages (hornblende + albite + epidote; Table 2) indicating top-(S)E shearing under epidote–amphibolite-facies conditions and possibly also higher-pressure conditions as suggested by the presence of glaucophane along shear bands. These are therefore attributed to deformation during exhumation of the UHP unit to lower crustal depths. The absence of kinematic indicators within eclogites in the surroundings of the sliver suggests that deformation during ascent of the Zermatt–Saas zone was localized at a different structural level, possibly the uppermost part which, however, has been strongly affected and overprinted by later retrogression and deformation. Lower-grade, i.e. greenschist-facies top-SE shear sense criteria, can be observed at higher structural levels above (U)HP rocks and are often associated with top-NW kinematic indicators. More importantly, this domain is characterized by significant coaxial deformation as documented by abundant conjugate sets of shear bands, symmetric fabrics, and boudinage. Replacement of white mica by chlorite along conjugate shear bands within partly retrogressed rocks as well as greenschist-facies symmetric fabrics within strongly retrogressed ones indicates greenschist-facies conditions during coaxial deformation. The different orientation of conjugate shear bands with respect to the greenschist-facies foliation and their often ‘post-chlorite’ character in some samples suggest that this event occurred after an initial phase of greenschist-facies deformation and retrogression along the top of the Zermatt–Saas zone. This deformation phase was possibly related to normal-sense top-SE shearing, continuing exhumation of the Zermatt–Saas zone at crustal levels, and juxtaposition with the overlying and strongly retrogressed greenschist-facies Combin zone. Top-SE structures are scarce within the Combin zone which may be due to localization of strain along the uppermost Zermatt–Saas zone so that the Combin Fault may have represented a decoupling surface during normal-sense shearing and ascent of (U)HP rocks in

its footwall. Additionally, exhumation-related deformation structures along the Combin Fault have most likely been overprinted by subsequent deformation phases. Coaxial deformation can be traced across the Combin Fault from the uppermost Zermatt–Saas zone into the lower Combin zone where it is preserved within quartzites of the Cimes Blanches nappe displaying orthorhombic textures and conjugate shear sense criteria as well as spatially associated top-NW and top-SE shear bands within Tsaté calcschists. Temperature estimates from *c*-axis opening angles in pole figures and observed SGR of quartz in thin section suggest conditions between ca. 400 and 450 °C for this phase. The similar style, geometry, and metamorphic grade of deformation in the immediate footwall and hanging wall of the Combin Fault suggest that the uppermost Zermatt–Saas zone and lowermost Combin zone experienced significant post-exhumational deformation and retrogression related to a phase of dominant pure shear. This deformational event after exhumation of (U)HP rocks to crustal levels and juxtaposition of the two units is interpreted to reflect NW–SE-directed crustal elongation. Despite the predominance of coaxial deformation along the Combin Fault, symmetric deformation structures often occur in association with top-NW kinematic indicators so that bulk top-NW shearing may have accompanied but also partly postdated pure shear deformation. The Tsaté nappe displays almost exclusively top-NW kinematic indicators which seem to be partly related to the main phase of greenschist-facies retrogression and fabric formation and partly to late and renewed top-NW shearing, which probably postdated pure shear deformation. The few observed top-SE to top-S kinematic indicators may reflect conjugate top-SE shearing or be related to normal-sense shearing during ascent of the Zermatt–Saas zone. Top-NW shear sense criteria are also abundant within mylonites along the DBBT and show a progressive decrease in metamorphic grade from high- to low-grade greenschist-facies conditions. Top-NW simple shear was the dominant deformation mechanism along the DBBT without any signs of a pure shear component or top-SE simple shear during ductile deformation. The decreasing metamorphic grade of kinematic indicators suggests that NW-vergent shearing occurred during several stages of the retrograde greenschist-facies evolution of the lower Dent Blanche nappe and can therefore be characterized as syn-exhumational. Main formation of greenschist-facies mylonitic fabrics along the DBBT may predate the observed pure shear deformation along the Zermatt–Saas/Combin boundary. Lower-grade top-NW kinematic indicators, on the other hand, most likely postdate this phase and are therefore ascribed to late-stage reactivation of the DBBT and renewed top-NW shearing which also affected the Tsaté nappe and partly units along the Combin Fault. Ductile top-NW shearing along the DBBT evolved into

semi-ductile to brittle top-NW deformation which in turn was followed by a minor phase of top-SE brittle faulting which can only locally be observed in the area around Lago di Cignana.

Our kinematic analyses and structural observations show that top-(S)E shearing under epidote–amphibolite-facies conditions was responsible for exhumation of UHP rocks to approximately lower crustal levels. Continuing exhumation of the Zermatt–Saas zone and juxtaposition with the overlying Combin zone most likely occurred during greenschist-facies top-SE shearing along the uppermost Zermatt–Saas zone and the Combin Fault. This phase was followed by post-exhumational, pure shear-dominated deformation, especially affecting the uppermost Zermatt–Saas zone and the lowermost Combin zone. The lower Dent Blanche nappe and partly the underlying Tsaté nappe show an evolution of prolonged or episodic top-NW shearing under decreasing metamorphic conditions. A first stage of foreland-directed top-NW shearing most likely accompanied exhumation of the Combin zone and Dent Blanche nappe to crustal levels and may have predated juxtaposition of the Combin and Zermatt–Saas zones. However, renewed top-NW shearing at higher structural levels also partly accompanied coaxial deformation along the Combin Fault and, more importantly, continued subsequently as suggested by low-grade greenschist-facies deformation structures along the DBBT.

### Previously published structural works

In this section, we compare our observations with existing structural works by other authors in the Lago di Cignana area. Ballèvre and Merle (1993) reported equally top-E and top-W shear sense criteria for Zermatt–Saas (U)HP rocks and therefore did not propose a bulk shear sense for deformation under (U)HP conditions or on the retrograde path after the peak of metamorphism. Van der Klauw et al. (1997) also reported rather conjugate sets of eclogite-facies shear bands and suggested that no considerable deformation was localized into metabasites during exhumation from UHP depths. The microstructural study by Müller and Compagnoni (2009) on the other hand showed that deformation of HP minerals occurred during all stages of the eclogite-facies evolution. Our study confirms the occurrence of top-(N)W shear sense criteria in addition to top-(S)E indicators in (U)HP rocks. However, we find a clear predominance of top-(S)E shear sense criteria within rocks of the UHP unit. Although some of them, especially within metasediments, cannot unambiguously be linked to deformation under (U)HP conditions or during subsequent retrogression, many of them show clear petrographic and microstructural evidence for deformation under retrograde epidote–amphibolite-facies conditions

and therefore during exhumation to approximately lower crustal levels. The strong greenschist-facies overprint in the uppermost Zermatt–Saas zone has already been recognized by Van der Klauw et al. (1997) who reported top-NW kinematic indicators along this domain in agreement with our observations. However, our analyses also show that top-NW shearing was preceded and accompanied by considerable portions of greenschist-facies coaxial deformation in the footwall and hanging wall of the Combin Fault indicating a dominant pure shear regime after juxtaposition of the Zermatt–Saas and Combin zones at crustal levels. Reddy et al. (2003) reported a dominant top-SE sense of shear for the Cimes Blanches nappe at Lago di Cignana. In contrast, our study revealed orthorhombic quartz textures and conjugate top-NNW and top-SSE kinematic indicators within quartzites suggesting dominant pure shear deformation in the direct hanging wall of the Combin Fault. Pleuger et al. (2007) analysed microstructures and textures of 3 Cimes Blanches quartzites from localities ca. 2 km NNE of Monte Seriola. They acquired top-NW as well as top-SE shear senses but attributed them to different stages of the greenschist-facies structural evolution instead of coaxial deformation. The observed pure shear deformation may have therefore been unequally distributed in the direct hanging wall of the Combin Fault in the Valtournenche area and may have been most pronounced at Lago di Cignana. Reddy et al. (2003) reported a predominance of top-NW kinematic indicators towards higher structural levels above the Cimes Blanches nappe at Lago di Cignana, which is confirmed by our study. Detailed mapping and structural work by Forster et al. (2004), especially within and around the UHP sliver, revealed a complex structural evolution of these units under (U)HP conditions. These authors reported older top-E kinematic indicators for Zermatt–Saas HP rocks overprinted by younger HP top-W and conjugate shear sense criteria, while for the UHP unit they reported dominant eclogite- to blueschist-facies top-(W)NW fabrics and kinematic indicators. These observations may indicate differential and faster exhumation of the UHP unit relative to surrounding HP rocks during (W)NW-directed thrusting under HP conditions. During this phase, normal-sense top-(S)E shearing may have been localized at a higher structural level, whereas it subsequently affected the UHP unit under epidote–amphibolite-facies conditions as suggested by our observations. Forster et al. (2004) also proposed a period of NW–SE-directed crustal extension after juxtaposition of the Zermatt–Saas and Combin zones, which led to crustal-scale boudinage and the development of conjugate shear zones. Such a phase would correspond to our postulated stage of post-exhumational pure shear deformation along the Combin Fault. Forster et al. (2004) suggested that all exposed units were already in a subhorizontal and partly NW- and SE-dipping position, respectively, after

exhumation to crustal levels. Reddy et al. (2003) also proposed that regional-scale folding was responsible for late reactivation of ductile shear zones in the Valtournenche area. We follow this interpretation and suggest that the observed phase of dominant pure shear deformation reflects NW–SE crustal elongation in response to updoming of the nappe stack.

### Structural evolution in the tectonic context of the Western Alps

In this section, we embed the results of our structural analyses into the tectonic framework of the Western Alps and propose a kinematic evolution for the units exposed at Lago di Cignana (Fig. 7).

The Zermatt–Saas zone probably experienced eclogite-facies conditions until ca. 41–40 Ma (Amato et al. 1999; Skora et al. 2015). Exhumation of UHP rocks from upper-mantle to lower crustal levels during normal-sense top-(S)E shearing under epidote–amphibolite-facies conditions is therefore interpreted to have occurred around 39 Ma (Fig. 7a). At that time, the Combin zone and Dent Blanche nappe were already largely exhumed to crustal levels and experienced a first phase of greenschist-facies top-(N)W deformation and retrogression (e.g. Reddy et al. 1999, 2003; Angiboust et al. 2014). Thrusting at higher crustal levels may have therefore prevailed, while ascent of the Zermatt–Saas zone at deeper levels occurred during normal-sense shearing (Fig. 7a). This overall geometry can best be explained by differential exhumation of the Zermatt–Saas zone with respect to the Combin zone and Dent Blanche nappe. Initial exhumation of the Zermatt–Saas zone from (U)HP conditions may have been triggered by buoyancy resulting from large portions of hydrated rock material (e.g. serpentinite, lawsonite eclogite; Angiboust and Agard 2010). Additionally, buoyancy of low-density, quartz-rich metasedimentary material of the UHP slice compared to surrounding mafic material probably led to differential and fast exhumation of this unit. (Ultra)high-pressure rocks at Lago di Cignana show the highest pressures and some of the youngest available ages related to eclogite-facies metamorphism in the Zermatt–Saas zone (Rubatto et al. 1998; Amato et al. 1999; Gouzu et al. 2006), suggesting that this unit was exhumed at higher rates than the surrounding HP rocks. Greenschist-facies retrogression within UHP rocks probably occurred around 38 Ma (Amato et al. 1999), which is interpreted to reflect the timing of juxtaposition with the overlying Combin zone during normal-sense top-SE shearing (Fig. 7b). Since ductile top-SE shear sense criteria are largely missing within the Combin zone and along the DBBT, normal-sense shearing is interpreted to have largely been localized along the uppermost Zermatt–Saas zone. A cluster of ages between ca. 39 and

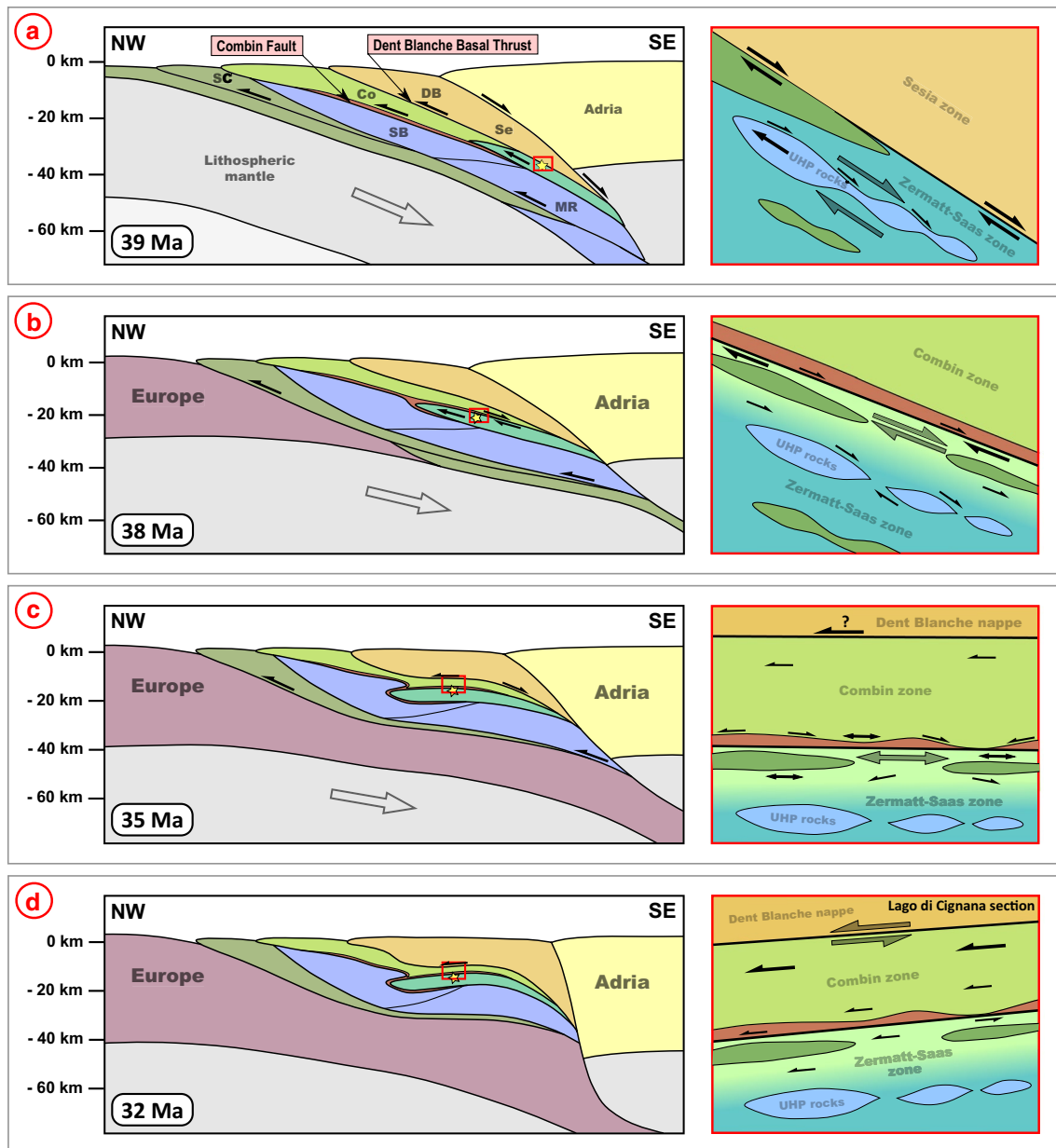


**Fig. 7** Tectonic evolution of the Western Alps with detail sketches of the structural and kinematic evolution of the upper Zermatt–Saas zone, the Combain zone, and the lower Dent Blanche nappe; red rectangles indicate areas of sketches on the right; large grey arrows indicate approximate domains of maximum strain during the respective deformation phase; sketches are not to scale; colour coding of tectonic sketches is the same as in Fig. 1, colours of detail sketches correspond to the ones in Fig. 2; yellow star indicates location of the Lago di Cignana UHP unit. **a** Situation at ca. 39 Ma: exhumation of Combain zone and Dent Blanche nappe at crustal levels during foreland-directed top-NW shearing along the Combain Fault and Dent Blanche Basal Thrust (DBBT); exhumation of Zermatt–Saas zone and associated UHP rocks to lower crustal levels during normal-sense top-(S)E shearing under epidote–amphibolite-facies conditions along its top; *DB* Dent Blanche nappe, *Se* Sesia nappe, *Co* Combain zone, *SB* St. Bernhard nappe system, *MR* Monte Rosa nappe, *SC* Zone of Sion-Courmayeur. **b** Situation at ca. 38 Ma: exhumation of Zer-

matt–Saas zone to mid-crustal levels and juxtaposition with overlying Combain zone along greenschist-facies top-SE shear zones. **c** Situation at ca. 35 Ma: dominant pure shear deformation under greenschist-facies conditions affecting units in the direct footwall and hanging wall of the Combain Fault and largely overprinting syn-exhumational deformation structures along the Combain Fault; this phase probably reflects NW–SE-directed crustal elongation resulting from updoming of the nappe stack due to underthrusting of European continental margin units and the onset of continental collision; it may have been accompanied by bulk top-NW shearing, especially at a higher structural levels and along the DBBT; large-scale folding of the nappe stack may have led to regional differences in the dominant vergence of shearing, i.e. top-NW in the western Valtourne and top-SE in the areas east of it. **d** Situation at ca. 32 Ma: renewed foreland-directed top-NW shearing as a result of continuing updoming led to reactivation and reworking of earlier structures

36 Ma associated with domains of dominant top-SE shear along the south-eastern segment of the Combin Fault has been reported by Reddy et al. (1999). Constraints on the timing of post-peak normal-sense shearing along the top of the Zermatt–Saas zone are also given by the age of retrograde top-SE shear zones formed between 42 and 37 Ma in the northeast close to the Mischabel fold (Cartwright and Barnicoat 2002). Formation of the Mischabel fold in the hanging wall of the northern Zermatt–Saas zone most likely represents a late stage of SE-vergent shearing at ca. 37 Ma after juxtaposition of the Combin and Zermatt–Saas zones (Barnicoat et al. 1995; Cartwright and Barnicoat 2002). While top-SE kinematic indicators are abundant in the areas southeast of Valtournenche, e.g. in the Val Gressoney area and along the Combin/Sesia contact (Wheeler and Butler 1993; Reddy et al. 1999; Pleuger et al. 2007, Gasco and Gattiglio 2011), the Combin zone in the western Valtournenche area is dominated by top-NW kinematic indicators (Ring 1995; Pleuger et al. 2007). It is often difficult to establish a relative chronology of deformation since all these structures formed under greenschist-facies conditions. On the basis of geochronological data, Reddy et al. (2003) proposed regional top-SE and top-NW shear zones overlapping in space and time due to a significant pure shear component and regional-scale folding. A similar scenario with conjugate shear zones during NW–SE-directed crustal extension and large-scale corrugation of the nappe stack has also been proposed by Forster et al. (2004) to explain the regional distribution of dominant shear senses. Large coaxial strains along the Combin Fault and within the Combin zone in the greater area have also been reported by Ring (1995) based on finite strain analyses and by Pleuger et al. (2007) on the basis of quartz texture analysis. Based on our structural observations and existing works, we favour a scenario in which juxtaposition of the Zermatt–Saas and Combin zones during top-SE normal-sense shearing at ca. 38 Ma was followed by a phase of NW–SE-directed crustal elongation with conjugate shear zones and pure shear deformation due to increasing updoming of the nappe stack in the Internal Western Alps (Fig. 7c). This phase most likely resulted from Late Eocene underthrusting of European continental margin units as indicated by prograde ages around 38–37 Ma within these units (Herwartz et al. 2011; Sandmann et al. 2014). Abundant shortening structures across the Alps and coarse clastic sedimentation in forelands for the period between ca. 38 and 34 Ma have been reported by Beltrando et al. (2010b) and also suggest an increased uplift of the nappe stack. The phase of dominant pure shear deformation is interpreted to have culminated at ca. 35 Ma and to have partly been accompanied by bulk top-NW shearing, probably due to ongoing or renewed foreland-directed movement of the Dent Blanche nappe (Fig. 7c). It was followed by more rotational NW-vergent

shearing after ca. 34 Ma (Fig. 7d) as evident from abundant low-grade greenschist-facies deformation structures. Late post-exhumational top-NW shearing has also been suggested by Ballèvre and Merle (1993) to explain the predominance of greenschist-facies top-NW kinematic indicators within the Combin zone. Following significant updoming, tectonic contacts and units in the western Valtournenche area probably had an already (sub)horizontal or possibly even NW-dipping orientation (Reddy et al. 2003; Forster et al. 2004). NW-vergent shearing during this phase therefore resulted either from low-angle thrusting or normal faulting (Fig. 7d). The geometry of post-exhumational top-NW shear zones and whether late foreland-directed shearing was reverse or normal sense cannot conclusively be resolved at this point. In contrast to observations from the Lago di Cignana and western Valtournenche area, top-SE shearing has been reported for the Tsaté nappe in the footwall of the north-western DBBT (Wust and Silverberg 1989; Reddy et al. 2003), suggesting that late NW-vergent shearing was not strictly parallel to tectonostratigraphy. Late greenschist-facies top-NW shearing overprinting earlier structures has not been reported for the areas southeast of Valtournenche where top-SE shearing seems to be the last deformational event (Wheeler and Butler 1993; Reddy et al. 2003; Babist et al. 2006; Pleuger et al. 2007, Gasco and Gattiglio 2011). Also, no greenschist-facies top-NW shear zone reemerging at a higher structural level in the Dent Blanche nappe has been reported so far. In contrast, Ballèvre and Merle (1993) proposed that a late top-NW ‘Combin Fault’ propagated down section into the St. Bernhard nappe system. Taking these constraints on shear zone geometry into account (see also Wheeler and Butler 1994), the observed top-NW shear zone probably rooted in an already eroded part of the Dent Blanche/Sesia nappe system and cut down section through the Combin zone and into the St. Bernhard nappe system. Continuing updoming of the Internal Western Alps, which transitioned into Vanzone phase folding from ca. 32 Ma onwards (e.g. Keller et al. 2005), is interpreted to have resulted in the observed top-NW brittle overprint along the DBBT.

## Conclusions

Kinematic analyses of shear zones at Lago di Cignana in the western Valtournenche of Italy constrain the structural evolution of the exposed units, the upper Zermatt–Saas zone, the Combin zone, and the lower Dent Blanche nappe, as well as the tectonic contacts separating them, the Combin Fault and the DBBT. Normal-sense top-(S)E shearing under epidote–amphibolite-facies conditions at ca. 39 Ma was responsible for exhumation of UHP

rocks to approximately lower crustal levels. Although syn-exhumational deformation structures are scarce along the Combin Fault, continuing exhumation of the Zermatt–Saas zone to mid-crustal levels and juxtaposition with the overlying Combin zone is inferred to have occurred during greenschist-facies top-SE shearing around 38 Ma. The scarcity of top-SE kinematic indicators in the hanging wall of the Combin Fault at Lago di Cignana and in the western Valtournenche area is interpreted to be the result of strain localization along the uppermost Zermatt–Saas zone during its ascent but also of obliteration by subsequent greenschist-facies deformation. A phase of dominant pure shear deformation at ca. 35 Ma affected units in the direct footwall and hanging wall of the Combin Fault. This phase is interpreted to reflect NW–SE crustal elongation due to underthrusting of European continental margin units, the onset of continental collision, and resulting updoming of the nappe stack. Dominant pure shear deformation along the Combin Fault probably occurred in a (sub)horizontal orientation of tectonic units and contacts. It was partly accompanied but more importantly followed by greenschist-facies top-NW shearing, especially at higher structural levels, which was related to either low-angle thrusting or normal faulting. This phase transitioned into Vanzone phase folding from ca. 32 Ma onwards resulting in semi-ductile to brittle reworking of the DBBT in the western Valtournenche area during normal-sense top-NW shearing. Our structural observations suggest that exhumation of UHP rocks and the upper Zermatt–Saas zone to crustal levels occurred during dominant normal-sense top-(S)E shearing, whereas the overlying Combin zone and lower Dent Blanche nappe experienced prolonged or episodic foreland-directed top-NW shearing under decreasing greenschist-facies conditions. A first stage of top-NW shearing may have been related to exhumation of the Combin zone and Dent Blanche nappe to crustal levels and predated juxtaposition of the Combin and Zermatt–Saas zones. However, syn-exhumational deformation structures along the Combin Fault and DBBT have been reworked and partly overprinted during post-exhumational coaxial deformation along the Combin Fault and renewed top-NW shearing along the DBBT.

**Acknowledgments** We thank Steven Reddy and an anonymous reviewer for their detailed and critical reviews which helped to significantly improve the manuscript. Comments by Walter Sullivan and an anonymous reviewer on an earlier version of the manuscript also helped to improve this work and are greatly acknowledged. We thank Rebecca Kühn for assistance with the X-ray texture goniometer at Geowissenschaftliches Zentrum Göttingen and Sebastian Weber for help in the field. We thank Thorsten Nagel for assistance with electron microprobe measurements, help in the field, and comments on an earlier version of this manuscript. This work was supported by scholarships from the University of Bonn and the Deutscher Akademischer Austauschdienst to FK as well as DFG grant FR 700/15-1.

## References

- Amato JM, Johnson CM, Baumgartner LP, Beard BL (1999) Rapid exhumation of the Zermatt–Saas ophiolite deduced from high-precision Sm–Nd and Rb–Sr geochronology. *Earth Planet Sci Lett* 171:425–438
- Angiboust S, Agard P (2010) Initial water budget: the key to detaching large volumes of eclogitized oceanic crust along a subduction channel? *Lithos* 120:453–474
- Angiboust S, Glodny J, Oncken O, Chopin C (2014) In search of transient subduction interfaces in the Dent Blanche–Sesia Tectonic System (W. Alps). *Lithos* 205:298–321
- Argand E (1906) Sur la tectonique du Massif de la Dent Blanche. *Comptes Rendus de l'Académie des Sciences Paris* 142:527–530
- Argand E (1909) L'exploration géologique des Alpes pennines centrales. *Bull Soc Vaud Sci Nat* 45:217–276
- Babist J, Handy MR, Konrad-Schmolke M, Hammerschmidt K (2006) Precollisional, multistage exhumation of subducted continental crust: the Sesia Zone, western Alps. *Tectonics* 25, TC6008. doi: [10.1029/2005TC001927](https://doi.org/10.1029/2005TC001927)
- Ballèvre M, Kienast JR (1987) Découverte et signification de paragenèses a grenat-amphibole bleu dans la couverture mésozoïque de la nappe de la Dent-Blanche (Alpes Occidentales). *Comptes Rendus de l'Académie des Sciences Paris* 305:43–46
- Ballèvre M, Merle O (1993) The combin fault: compressional reactivation of a late cretaceous-early tertiary detachment fault in the Western Alps. *Schweiz Mineral Petrograph Mitt* 73:205–227
- Ballèvre M, Kienast JR, Vuichard JP (1986) La “nappe de la Dent-Blanche” (Alpes occidentales): deux unités austroalpines indépendantes. *Eclogae Geol Helv* 79:57–74
- Barnicoat AC, Rex DC, Guise PG, Cliff RA (1995) The timing of and nature of greenschist facies deformation and metamorphism in the upper Pennine Alps. *Tectonics* 14:279–293
- Bearth P (1967) Die Ophiolite der Zone von Zermatt–Saas Fee. *Beitr Geol Karte Schweiz* 132:1–130
- Beltrando M, Rubatto D, Manatschal G (2010a) From passive margins to orogens: the link between ocean-continent transition zones and (ultra)high-pressure metamorphism. *Geology* 38:559–562
- Beltrando M, Lister GS, Rosenbaum G, Richards S, Forster M (2010b) Recognizing episodic lithospheric thinning along a convergent plate margin: the example of the Early Oligocene Alps. *Earth Sci Rev* 103:81–98
- Beltrando M, Manatschal G, Mohn G, Dal Piaz GV, Vitale Brovarone A, Masini E (2014) Recognizing remnants of magma-poor rifted margins in high-pressure orogenic belts. *Earth Sci Rev* 131:88–115
- Bousquet R (2008) Metamorphic heterogeneities within a single HP unit: overprint effect or metamorphic mix? *Lithos* 103:46–69
- Bowtell SA, Cliff RA, Barnicoat AC (1994) Sm–Nd isotopic evidence on the age of eclogitization in the Zermatt–Saas ophiolite. *J Met Geol* 12:187–196
- Bucher K, Fazis Y, de Capitani C, Grapes R (2005) Blueschists, eclogites, and decompression assemblages of the Zermatt–Saas ophiolite: high-pressure metamorphism of subducted Tethys lithosphere. *Am Mineral* 90:821–835
- Bussy F, Venturini G, Hunziker JC, Martinotti G (1998) U–Pb ages of magmatic rocks of the Western Austroalpine Dent-Blanche–Sesia unit. *Schweiz Mineral Petrograph Mitt* 78:163–168
- Caby R (1981) Le Mésozoïque de la zone du Combin en Val d'Aoste (Alpes graies): imbrications tectonique entre séries issues des domaines pennique, austroalpin et océanique. *Géol Alp* 57:5–13
- Cartwright I, Barnicoat AC (2002) Petrology, geochronology, and tectonics of shear zones in the Zermatt–Saas and Combin zones of the Western Alps. *J Met Geol* 20:263–281

- Ciarapica G, Dal Piaz GV, Passeri L (2010) Late Triassic microfossils in the Roisan zone, Austroalpine Dent Blanche-Mont Mary nappe system, NW-Alps. *Rendic Online Soc Geol Ital* 11:261
- Dal Piaz GV (1965) La formation mesozoica dei calcescisti con pietre verdi fra la Valsesia e la Valtournanche ed i suoi rapporti strutturali con il recoprimento Monte Rosa e con la Zona Sesia–Lanzo. *Boll Soc Geol Ital* 84:67–104
- Dal Piaz GV (1999) The Austroalpine–Piedmont nappe stack and the puzzle of Alpine Tethys. *Mem Sci Geol* 51:155–176
- Dal Piaz GV, Ernst WG (1978) Areal geology and petrology of eclogites and associated metabasites of the Piemonte Ophiolite Nappe, Breuil-St. Jacques, Italian Western Alps. *Tectonophysics* 51:99–126
- Dal Piaz GV, Cortiana G, Del Moro A, Martin S, Pennacchioni G, Tartarotti P (2001) Tertiary age and paleostructural inferences of the eclogitic imprint in the Austroalpine outliers and Zermatt–Saas ophiolite, western Alps. *Int J Earth Sci* 90:668–684
- De Meyer CMC, Baumgartner LP, Beard BL, Johnson CM (2014) Rb–Sr ages from phengite inclusions in garnets from high pressure rocks of the Swiss Western Alps. *Earth Planet Sci Lett* 395:205–216
- Escher A, Masson H, Steck A (1993) Nappe geometry in the Western Alps. *J Struct Geol* 15:501–509
- Escher A, Hunziker JC, Marthaler M, Masson H, Sartori M, Steck A (1997) Geologic framework and structural evolution of the western Swiss-Italian Alps. In: Pfiffner OA, Lehner P, Heitzmann P, Müller S, Steck A (eds) *Deep structure of the Swiss Alps - results from NRP 20*. Birkhäuser, Basel, pp 205–221
- Fassmer K, Obermüller G, Nagel TJ, Kirst F, Froitzheim N, Sandmann S, Miladinova I, Fonseca ROC, Münker C (2016) High-pressure metamorphic age and significance of eclogite-facies continental fragments associated with oceanic lithosphere in the Western Alps (Etirol-Levaz Slice, Valtournanche, Italy). *Lithos*. doi:10.1016/j.lithos.2016.02.019
- Forster M, Lister G, Compagnoni R, Giles D, Hills Q, Betts P, Beltrando M, Tamagno E (2004) Mapping of oceanic crust with “HP” to “UHP” metamorphism: The Lago di Cignana Unit (Western Alps). In: Pasquarè G, Venturini C, Groppelli G (eds) *Mapping geology in Italy*, Servizio Geologico d’Italia, Roma, pp 279–286
- Frezzotti ML, Selverstone J, Sharp ZD, Compagnoni R (2011) Carbonate dissolution during subduction revealed by diamond-bearing rocks from the Alps. *Nat Geosci* 4:703–706
- Froitzheim N (2001) Origin of the Monte Rosa nappe in the Pennine Alps—a new working hypothesis. *GSA Bull* 113:604–614
- Froitzheim N, Schmid SM, Frey M (1996) Mesozoic paleogeography and the timing of eclogite-facies metamorphism in the Alps: a working hypothesis. *Eclogae Geol Helv* 89:81–110
- Froitzheim N, Pleuger J, Nagel TJ (2006) Extraction faults. *J Struct Geol* 28:1388–1395
- Gardien V, Reusser E, Marquer D (1994) Pre-Alpine metamorphic evolution of the gneisses from Valpelline series (Western Alps, Italy). *Schweiz Mineral Petrograph Mitt* 74:489–502
- Gasco I, Gattiglio M (2011) Geological map of the upper Gressoney Valley, Western Italian Alps. *J Maps*. doi:10.4113/jom.2011.1121
- Gouzu C, Itaya T, Hyodo H, Matsuda T (2006) Excess <sup>40</sup>Ar-free phengite in ultrahigh-pressure metamorphic rocks from the Lago di Cignana area, Western Alps. *Lithos* 92:418–430
- Groppo C, Beltrando M, Compagnoni R (2009) The P–T path of the ultra-high pressure Lago di Cignana and adjoining meta-ophiolitic units: insights into the evolution of the subducting Tethyan slab. *J Met Geol* 27:207–231
- Handy MR, Schmid SM, Bousquet R, Kissling E, Bernoulli D (2010) Reconciling plate-tectonic reconstructions of Alpine Tethys with the geological-geophysical record of spreading and subduction in the Alps. *Earth Sci Rev* 102:121–158
- Herwartz D, Nagel TJ, Münker C, Scherer EE, Froitzheim N (2011) Tracing two orogenic cycles in one eclogite sample by Lu–Hf garnet chronometry. *Nat Geosci* 4:178–183
- Inger S, Ramsbotham W, Cliff RA, Rex DC (1996) Metamorphic evolution of the Sesia–Lanzo Zone, Western Alps: time constraints from multi-system geochronology. *Contrib Mineral Petrol* 126:152–168
- Keller LM, Schmid SM (2001) On the kinematics of shearing near the top of the Monte Rosa nappe and the nature of the Furgg zone in Val Loranco (Antrona valley, N. Italy): tectonometamorphic and paleogeographic consequences. *Schweiz Mineral Petrograph Mitt* 81:347–367
- Keller LM, Hess M, Fügenschuh B, Schmid SM (2005) Structural and metamorphic evolution of the Camughera–Moncucco, Antrona and Monte Rosa units southwest of the Simplon line, Western Alps. *Eclogae Geol Helv* 98:19–49
- Kruhl JH (1996) Prism- and basal-plane parallel subgrain boundaries in quartz: a microstructural geothermobarometer. *J Met Geol* 14:581–589
- Lapen TJ, Johnson CM, Baumgartner LP, Mahlen NJ, Beard BL, Amato JM (2003) Burial rates during prograde metamorphism of an ultrahigh-pressure terrane: an example from Lago di Cignana, Western Alps, Italy. *Earth Planet Sci Lett* 215:57–72
- Lardeaux JM, Spalla MI (1991) From granulites to eclogites in the Sesia Zone (Italian Western Alps), a record of opening and closure of the Piedmont ocean. *J Met Geol* 9:35–59
- Law RD, Searle MP, Simpson RL (2004) Strain, deformation temperatures and vorticity of flow at the top of the Greater Himalayan Slab, Everest Massif, Tibet. *J Geol Soc Lond* 161:305–320
- Mahlen NJ, Skora S, Johnson CM, Baumgartner LP, Lapen TJ, Skora S, Beard BL, Pilet S (2005) Lu–Hf geochronology of eclogites from Pfulwe, Zermatt–Saas Ophiolite, western Alps, Switzerland. *Geochim Cosmochim Acta* 69:A305
- Manzotti P (2011) Petro-structural map of the Dent Blanche tectonic system between Valpelline and Valtournanche valleys, Western Italian Alps. *J Maps*. doi:10.4113/jom.2011.1179
- Manzotti P, Zucali M, Ballèvre M, Robyr M, Engi M (2014) Geometry and kinematics of the Roisan–Cignana Shear Zone, and the orogenic evolution of the Dent Blanche Tectonic System (Western Alps). *Swiss J Geosci* 107:23–47
- Marthaler M, Stampfli GM (1989) Les Schistes lustrés à ophiolites de la nappe du Tsaté: un ancien prisme d’accrétion issu de la marge active apulienne? *Schweiz Mineral Petrograph Mitt* 69:211–216
- Mazurek M (1986) Structural evolution and metamorphism of the Dent Blanche nappe and the Combin zone west of Zermatt (Switzerland). *Eclogae Geol Helv* 79:41–56
- Monjoie P, Bussy F, Lapierre H, Pfeifer HR (2005) Modeling of in situ crystallization processes in the Permian mafic layered intrusion of Mont Collon (Dent Blanche nappe, western Alps). *Lithos* 83:317–346
- Müller WF, Compagnoni R (2009) Eclogite from the ultrahigh-pressure metamorphic unit at Lago di Cignana, Western Alps: a process-oriented transmission electron microscope study. *Lithos* 109:323–332
- Negro F, Bousquet R, Vils F, Pellet CM, Hänggi-Schaub J (2013) Thermal structure and metamorphic evolution of the Piemont–Ligurian metasediments in the northern Western Alps. *Swiss J Geosci* 106:63–78
- Oberhänsli R, Bucher K (1987) Tectonometamorphic evolution of the Dent Blanche nappe. *Terra Cognita* 7(2-3):95
- Pleuger J, Froitzheim N, Jansen E (2005) Folded continental and oceanic nappes on the southern side of Monte Rosa (western Alps, Italy): anatomy of a double collision suture. *Tectonics* 24, TC4013. doi:10.1029/2004TC001737
- Pleuger J, Roller S, Walter JM, Jansen E, Froitzheim N (2007) Structural evolution of the contact between two Penninic nappes

- (Zermatt–Saas zone and Combin zone, Western Alps) and implications for the exhumation mechanism and paleogeography. *Int J Earth Sci* 96:229–252
- Pryer LL (1993) Microstructures in feldspars from a major crustal thrust zone: the Grenville Front, Ontario, Canada. *J Struct Geol* 15:21–36
- Reddy SM, Wheeler J, Cliff RA (1999) The geometry and timing of orogenic extension: an example from the Western Italian Alps. *J Met Geol* 17:573–589
- Reddy SM, Wheeler J, Butler RWH, Cliff RA, Freeman S, Inger S, Pickles C, Kelley SP (2003) Kinematic reworking and exhumation within the convergent Alpine Orogen. *Tectonophysics* 365:77–102
- Regis D, Rubatto D, Darling J, Cenko-Tok B, Zucali M, Engi M (2014) Multiple metamorphic stages within an eclogite-facies terrane (Sesia Zone, Western Alps) revealed by Th–U–Pb petrochronology. *J Petrol* 55:1429–1456
- Reinecke T (1991) Very-high-pressure metamorphism and uplift of coesite-bearing metasediments from the Zermatt–Saas zone, Western Alps. *Eur J Mineral* 3:7–17
- Reinecke T (1998) Prograde high- to ultrahigh-pressure metamorphism and exhumation of oceanic sediments at Lago di Cignana, Zermatt–Saas Zone, western Alps. *Lithos* 42:147–189
- Ring U (1995) Horizontal contraction or horizontal extension? Heterogeneous Late Eocene and Early Oligocene general shearing during blueschist and greenschist facies metamorphism at the Pennine–Austroalpine boundary zone of the Western Alps. *Geol Rundsch* 84:843–859
- Rubatto D, Gebauer D, Fanning M (1998) Jurassic formation and Eocene subduction of the Zermatt–Saas–Fee ophiolites: implications for the geodynamic evolution of the Central and Western Alps. *Contrib Mineral Petrol* 132:269–287
- Rubatto D, Gebauer D, Compagnoni R (1999) Dating of eclogite-facies zircons: the age of Alpine metamorphism in the Sesia–Lanzo zone (western Alps). *Earth Planet Sci Lett* 167:141–158
- Rubatto D, Regis D, Hermann J, Boston K, Engi M, Beltrando M, McAlpine SRB (2011) Yo-yo subduction recorded by accessory minerals in the Italian Western Alps. *Nat Geosci* 4:338–342
- Sandmann S, Nagel TJ, Herwardt D, Fonseca ROC, Kurzwski RM, Münker C, Froitzheim N (2014) Lu–Hf garnet systematics of a polymetamorphic basement unit: new evidence for coherent exhumation of the Adula Nappe (Central Alps) from eclogite-facies conditions. *Contrib Mineral Petrol* 168:1075
- Sartori M (1987) Structure de la zone du Combin entre les Diablos et Zermatt (Valais). *Eclogae Geol Helv* 80:789–814
- Schmid SM, Casey M (1986) Complete fabric analysis of some commonly observed quartz c-axis patterns. In: Hobbs BE, Heard HC (eds) *Mineral and rock deformation: laboratory studies: the Paterson volume*. Geophysical Monograph Series, vol 36. American Geophysical Union, Washington, DC, pp 263–286
- Schmid SM, Fügenschuh B, Kissling E, Schuster R (2004) Tectonic map and overall architecture of the Alpine orogen. *Eclogae Geol Helv* 97:93–117
- Skora S, Mahlen NJ, Johnson CM, Baumgartner LP, Lapen TJ, Beard BL, Szilvagy ET (2015) Evidence for protracted prograde metamorphism followed by rapid exhumation of the Zermatt–Saas Fee ophiolite. *J Met Geol* 33:711–734
- Stampfli GM, Borel GD, Marchant R, Mosar J (2002) Western Alps geological constraints on western Tethyan reconstructions. *J Virtual Explorer* 8:77–106
- Steck A, Bigioggero B, Dal Piaz GV, Escher A, Martinotti G, Masson H (1999) Carte tectonique des Alpes de Suisse occidentale et des régions avoisinantes 1:100.000, Carte spèc. n. 123 (4 maps). Serv. Hydrol. Géol. Nat., Bern
- Stipp M, Stünitz H, Heilbronner R, Schmid SM (2002) The eastern Tonalite fault zone: a “natural laboratory” for crystal plastic deformation of quartz over a temperature range from 250 to 700°C. *J Struct Geol* 24:1861–1884
- Tamagno E (2000) L’unità meta-ofilologica di pressione molto alta del Lago di Cignana (Valtournenche—Aosta) e le sue relazioni con le unità tettoniche vicine. M.Sc. thesis, University of Torino, Italy
- Van der Klauw SNGC, Reinecke T, Stöckhert B (1997) Exhumation of ultrahigh-pressure metamorphic oceanic crust from Lago di Cignana, Piemontese zone, western Alps: the structural record in metabasites. *Lithos* 41:79–102
- Vannay JC, Allemann R (1990) La Zone Piémontaise dans le Haut-Valtournanche (Val d’Aoste, Italie). *Eclogae Geol Helv* 83:21–39
- Weber S, Sandmann S, Miladinova I, Fonseca ROC, Froitzheim N, Münker C, Bucher K (2015) Dating the initiation of Piemonte–Liguria Ocean subduction: Lu–Hf garnet chronometry of eclogites from the Theodul Glacier Unit (Zermatt–Saas Zone, Switzerland). *Swiss J Geosci*. doi:10.1007/s00015-015-0180-5
- Wheeler J, Butler RWH (1993) Evidence for extension in the western Alpine orogen: the contact between the oceanic Piemonte and overlying continental Sesia units. *Earth Planet Sci Lett* 117:457–474
- Wheeler J, Butler RWH (1994) Criteria for identifying structures related to true crustal extension in orogens. *J Struct Geol* 16:1023–1027
- Wheeler J, Reddy SM, Cliff RA (2001) Kinematic linkage between internal zone extension and shortening in more external units in the NW Alps. *J Geol Soc* 158:439–443
- Wust GS, Silverberg DS (1989) Northern Combin zone complex—Dent Blanche nappe contact: extension within the convergent Alpine belt. *Schweiz Mineral Petrogr Mitt* 69:251–259